Universidade de Aveiro Departamento de Química
Ano 2011

BINH XUAN VU

Encapsulação de nanopartículas utilizando agentes RAFT do tipo PAA e PEGA

Encapsulation of nanoparticles using PAA and PEGA macroRAFT agents

Universidade de Aveiro Departamento de Química
Ano 2011

BINH XUAN VU

Encapsulação de nanopartículas utilizando agentes RAFT do tipo PAA e PEGA

Encapsulation of nanoparticles using PAA and PEGA macroRAFT agents

Dissertação apresentada à Universidade de Aveiro para cumprimento dos requisitos necessários à obtenção do grau de Mestre em Ciência dos Materiais mestrado), realizada sob a orientação científica do Dra. Ana Barros Timmons, Professor Auxiliar do Departamento de Química da Universidade de Aveiro

o júri

presidente

Prof. Dr. Florinda Mendes da Costa
Associate Professor, Universidade de Aveiro

Prof. Dr. Maria Do Rosário Ribeiro
Auxiliary Professor, Universidade Tecnica de Lisboa

Prof. Dr. Ana Magarida Madeira Viegas de Barros Timmons
Auxiliary Professor, Universidade de Aveiro

Acknowledgment

I would like to express my greatful thank to my supervisor, Professor Ana Barros Timmons for her tireless support and guidance throughout my thesis.

I would like to thank Professor Dmitri for his assistance concerning GPC. I also would like to thank Celeste for helping me with the furnace and FT-IR. My thanks also to Sandra for her assistance with DMA. Thanks to Marta, Ricardo, Lisendra for their help with SEM. I am also greatful to Nuno, Belinda, Andreia, Carla for their assistance in the laboratory. Finally, I would like to thank the European Commision for financing my Master Course through EMMS Erasmus Mundus Programme.

palavras-chave

Agentes RAFT macromoleculares, polimerização em emulsão, encapsulação, nanocompósitos

Resumo

O bom desempenho dos nanocompósitos híbridos de matriz polimérica (NCs) requer uma dispersão homogénea das nanopartículas inorgânicas (NPs) de modo a garantir boa interacção entre as fases orgânica e inorgânica. Apesar de existirem já vários métodos de preparação deste tipo de NCs, nomeadamente através da técnica de polimerização em emulsão, subsistem ainda limitações. No sentido de as ultrapassar, a utilização de agentes RAFT macromoleculares tem recentemente vindo a ser explorada.

Numa primeira fase deste trabalho foram preparados quatro agentes RAFT macromoleculares com diferentes tamanhos de cadeia e composições através da polimerização do ácido acrílico (AA) e de acrilato de poli(etileno glicol)metil éter (PEGA) em solução usando como agente RAFT o ácido 2-{[(dodeciltio)carbonotioil]tio] -2- metilpropanóico (TTCA). Os polímeros obtidos foram caracterizados por espectroscopia de infravermelhos com transformadas de Fourier (FT-IR) e de ressonância magnética nuclear de protão (^{1}H-NMR), bem como a cromatografia de permeação de gel (GPC). Os agentes RAFT macromoleculares foram depois utilizados para preparar co-polímeros de bloco com *n*-acrilato de butilo (BA) por polimerização em emulsão. Os co-polímeros resultantes foram caracterizados por ^{1}H-NMR, FT-IR, GPC e DMA. A sensibilidade dos co-polímeros à base de PAA ao pH foi avaliada através de medições de tamanho de partícula e de potencial zeta em função do pH. No que concerne a estabilidade coloidal, avaliada por dispersão dinâmica de luz (DLS), verificou-se que os co-polímeros preparados utilizando o P(PEGA)-TTC deram origem a sistemas coloidais mais estáveis do que os preparados utilizando o PAA-TTC.

Por fim, foram preparados vários NCs utilizando NPs de sílica previamente modificada e nanofios (NWs) de óxido de zinco. Uma vez que os NWs obtidos apresentaram problemas de agregação o seu uso foi descontinuado. Os NCs foram caracterizados por FT-IR, DMA, DLS e SEM tendo-se confirmado o encapsulamento em todos os casos. O uso de agentes RAFT macromoleculares à base de PEGA parece dar origem a látexes estáveis do o uso de agentes macromoleculares à base de PAA. Porém os resultados de SEM e DLS apontam para a necessidade de melhoriras nos dois casos. No caso dos NCs preparados à base de PAA, a presença de uma coroa sensível ao pH foi confirmada através de medições de DLS e potencial zeta em função do pH.
Os resultados de DMA indicam uma tendência para a miscibilidade dos blocos de PAA e do PBA que reduz no caso dos NCs proventura devido à maior interacção do bloco de PAA com as NPs. No caso dos sistemas preparados com P(PEGA) a miscibilidade não é tão significativa.

keywords macroRAFT agents, emulsion polymerization, encapsulation, nanocomposites.

abstract

The performance of organic polymer-inorganic nanocomposites (NCs) depends on the homogenous dispersion of the inorganic nanoparticles (NPs) to ensure strong interaction between the nanofillers and the polymer matrix. Although a variety of methods already exists, current encapsulation techniques through emulsion polymerization suffer from several limitations. In order to overcome such limitations the use of amphiphilic macroRAFT agents is recently being explored.

In the present work macroRAFT agents with different chain lengths and composition were initially prepared by solution polymerization of acrylic acid (AA), poly(ethylene glycol) methyl ether acrylate (PEGA) and a combination of the two using (2-(docdecylthiocarbonothioylthio)-2-methyl propanoic acid (TTC-A) as the chain transfer agent. The macroRAFT agents obtained were characterized by proton nuclear magnetic resonance (^{1}H-NMR) and Fourier transform infrared (FT-IR) spectroscopies and Gel Permeation Chromatography (GPC) confirmed their successful synthesis. These Macro RAFT agents were then used prepare block copolymers with butyl acrylate via emulsion polymerization. The ensuing materials were characterized by 1H-NMR, FT-IR, Dynamic Mechanical Analysis (DMA) and GPC. Zeta potential measurements as a function of pH confirmed the pH-responsive behaviour of the PAA based systems whilst dynamic light scattering (DLS) measurements showed that the use of P(PEGA)-TTC provides better colloidal stability then the use of PAA-TTC

Finally, NCs were prepared using previously modified silica NPs and ZnO nanowires (NWs) as nanofillers. ZnO NWs were only used with the PAA system since it was concluded that the method used for their preparation yielded NWs that were still aggregated. Encapsulation of the NPs was confirmed by FT-IR, DMA, SEM and DLS. The latexes prepared using PEGA based systems seem to be more stable than those prepared with PAA. Yet, the SEM and DLS results prove that both systems require improvement. The presence of a polymeric stimuli – responsive shell covering the inorganic NPs using PAA-TTC was proved by DLS and Zeta potential measurements as a function of pH.

The DMA results suggest that the PAA and PBA blocks tend to blend but when NPs are present that miscibility is reduced possibly due to the interaction between the PAA groups and the NPs surface. For the P(PEGA) based systems the miscibility between the polymer blocks is not so relevant.

Contents

List of Figures, Schemes and Tables

List of Abbreviations

AA	Acrylic Acid
ATRP	Atom Transfer Radical Polymerizaton
BuA	Butyl Acrylate
CRP	Controlled Radical Polymerization
DLS	Diffusion Light Scattering
DMA	Dynamic Mechanical Analysis
DMF	Dimethylformamide
FT-IR	Fourier Transform Infrared Spectroscopy
GPC	Gel Permeation Chromatoraphy
LRP	Living Radical Polymerization
Mn	Number Average Molecular Weight
Mw	Weight Average Molecular Weight
NMP	NitroxideMediated Polymerization
NMR	Nulear Magnetic Resonance
PAA	Poly(Acrylic acid)
PBuA	Poly(Butyl acrylate)
PEGA	Poly (ethylene glycol) methyl ether acrylate
PMMA	Poly (methyl methacrylate)
PDI	Polydisperisty Index
RAFT	Reversible Addition Fragmentation Chain Transfer
SEM	Scanning Electron Microscopy
TEM	Transmisson Electron Microscopy
TEOS	Tetra-ethylorthosilicate
Tg	Glass Transition Temperature
THF	Tetrahydrofuran

1. INTRODUCTION

1.1. Nanocomposite – hybrid materials

Nanocomposites are a relatively new type of materials in which one component has at least one of its dimensions at nano scale. The properties of a nanocomposite material like any composite materials are the combination of the fillers and the matrix properties. Moreover, beyond the heritage from the parent properties, composite materials also exhibit novel characteristics which are not based on identified properties of separated components. Novel properties are the results of the morphology and the interfacial interaction between the fillers and the matrix.

Nanocomposite materials are divided in three main groups based on the nature of the constituents which can be organic or inorganic. They are organic/organic, inorganic/organic and inorganic/inorganic. Among these nanocomposite families, this study only focuses on polymer/inorganic consisting of nano-sized inorganic fillers distributed in a polymer matrix [1].

1.2. Polymer matrix preparation using RAFT Living polymerization

Traditional free radical polymerization has been used as a commercial process for the production of a vast family of polymers which is used to prepare composites due to the mild conditions required and high compatibility with many monomers and fillers. However, free radical polymerization or non-living polymerization still face many challenges in controlling many of the key factors such as molecular weight, polydispersity, ability to synthesize block copolymers with innovative structures or functional group attachment on the polymer chain. These disadvantages are the result of the uncontrolled termination of the chains during the polymerization process. By using controlled/living polymerization technique, one is allowed to produce polymers with predetermined molecular weights with narrow molecular weight distribution as well as succeeding in preparing novel architectures such as block copolymers, star polymers, branched polymers as illustrated in Figure 1 [2].

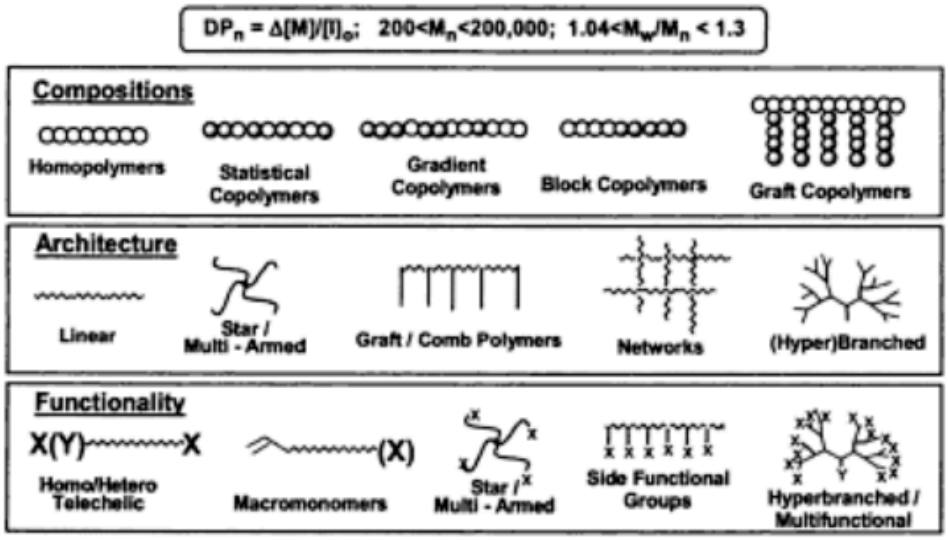

Figure 1: Polymer morphologies by control radical polymerization [2]

The livingness of the polymerization is defined as the continuous chain growth in the presence of the monomers without unexpected termination. Three widely used approaches of nowadays living radical polymerization include: a) Nitroxide-meditated method (NMP); b) Atom transfer radical polymerization (ATRP) and c) reversible addition-fragmentation chain transfer (RAFT). The principle of these methods lies on a dynamic equilibrium between the active free radicals and the dormant complexes. Each of the three techniques has been extensively investigated to synthesize polymers matrixes for nanocomposites. In this work, only RAFT technique is considered.

Among all living radical polymerization methods, RAFT is the most recently developed living radical polymerization technique which was invented in 1998 by a group in Australia (SCIRO) [3]. Different from NMP and ATRP which are based on the reversible equilibrium between the active species and a dormant agent- a termination of the active growing chain process, the principle of RAFT relies on a reversible addition - fragmentation balance. The mechanism of the process is illustrated in Scheme 1.

Pre-equilibrium:

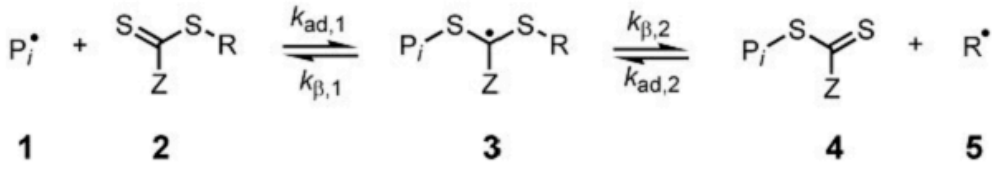

Main equilibrium:

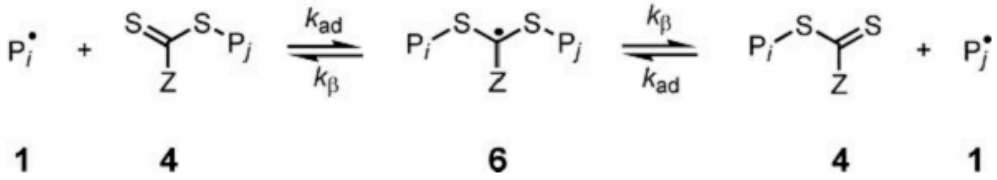

Scheme 1: Basic steps of the RAFT processes occurring in dithioester-mediated radical polymerization [3].

The RAFT method has been used to prepare a wide range of polymeric systems such as styrene [4-10], methacrylate [7], acrylamide [11] and acrylate [8, 11-18]. In view of the advantages of RAFT such as the use of simple compound and convenient working temperature, in our study, RAFT was used to prepare polymer matrix for the encapsulation of silica and ZnO nanoparticles.

1.2.1. RAFT agents

The controlling agent of the process is called RAFT agent which has the general formula of 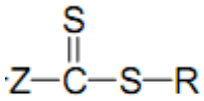 which is a dithioester compound. In the pre- equilibrium when a propagating chain comes to react with the agent, the radical is transferred to the agent to produce an intermediate carbon-centered radical. This intermediate can either fragment to produce the original radical species and the RAFT agent; or it can liberate the leaving group with a new carbon – centered radical (R^*). This leaving group, R^*, reacts with monomers forming a new propagating chain. Eventually, a balance between the propagating chain (1) and the dormant poly-RAFT agent (4) is established.

A RAFT agent is comprised of a reactive double bond C=S, a weak single bond S-R with Z is a group which determines the addition and fragmentation rates, R is a free radical leaving group. After release, R^* must be able to initiate polymerization. The compounds found to be suitable for this purpose include aromatic and aliphatic dithioesters, trithiocarbonates, dithiocarbamates and xanthates. The selection of proper RAFT agent depends strongly on the nature of the monomers to be polymerized. The guideline of selection of Z and R groups can depending on the particular monomers is presented in Figure 2.

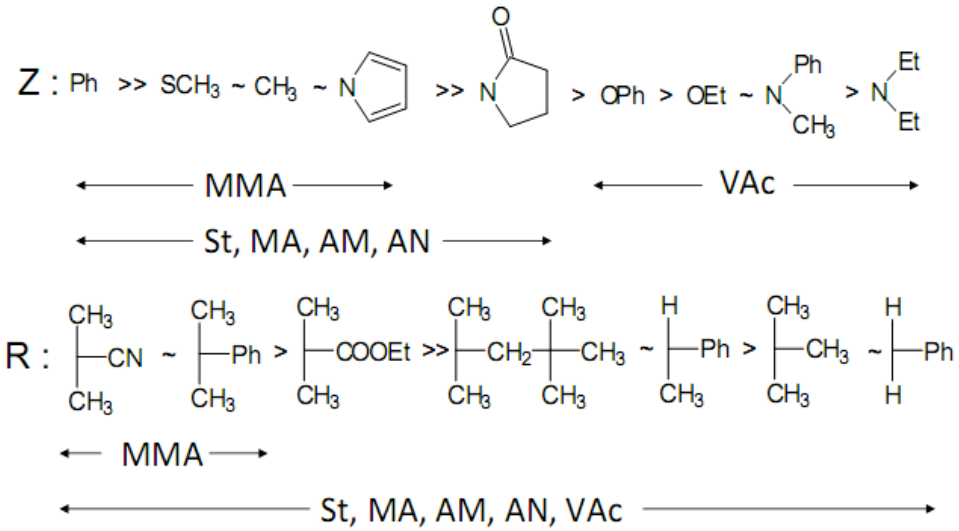

Figure 2: Guideline in selection of RAFT agent [3]. MMA-Methyl Methacrylate; VAc-Vinyl Acetate; St-Styrene; MA-Methyl acrylate; AM-Acrylamine; AN-Acrylonitrile

For Z group, from left to right, the rate of addition decreases while the rate of fragmentation increases. For R group, from left to right, the rate of fragmentation decreases and the rate of addition increases.

In our study, we made use of one RAFT agent which is a trithiocarbonate: 2-(dodecylthiocarbonothioylthio)-2-me-thylpropanoic acid) (TTCA). The structure of the agent is shown in Figure 3.

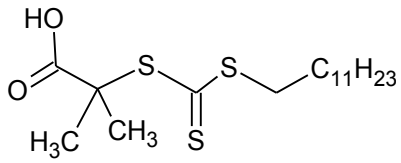

R: $-C(CH_3)_2COOH$

Z: $-SC_{11}H_{23}$

Figure 3: TTC-A as a RAFT agent

TTC-A is comprised of a hydrophobic dodecyl part and a hydrophilic carboxylic acid part. The amphiphilic nature makes TTC-A not only a chain transfer agent but also a stabilizer suitable to be used in emulsion polymerization.

1.2.2. MacroRAFT agents

Using conventional RAFT agents has encountered several difficulties when preparing block copolymers or when processing in heterogeneous conditions associated with low colloidal stability, poor control of molar mass and high polydispersity index. The solution for this is to use miniemulsion, seeded emulsion [9] polymerization or use conventional surfactants or stabilizers such as sodium dodecyl sufate(SDS) or cetyltrimethylammonium bromide. However, miniemulsion has been found to be too drastic for RAFT polymerization; seeded emulsion polymerization had problems with retardation and inhibition effect; and conventional surfactants are difficult to remove from the reaction mixture. A novel approach involves the use of macromolecular RAFT agent. A macroRAFT agent is composed of a polymeric part and a reactive RAFT agent part. The polymeric part may be formed by performing a polymerization using RAFT agent as the control agent or can be formed by chemically attaching the already formed polymer chain to the RAFT agent through proper chemical process. Ferguson et al. [14, 18, 19] introduced a technique to prepare macroRAFT agents which is illustrated in Scheme 2. In this approach the macroRAFT agent is comprised of a hydrophilic acrylic acid chain and an hydrophobic butylacrylate chain. The amphiphilic macroRAFT agent was synthesized by sequential addition of two types of monomer. The as-formed macroRAFT agent will self-assemble to form micelles in the water medium. The subsequent addition of a third monomer such as styrene would form novel core-shell polymeric nanoparticles.

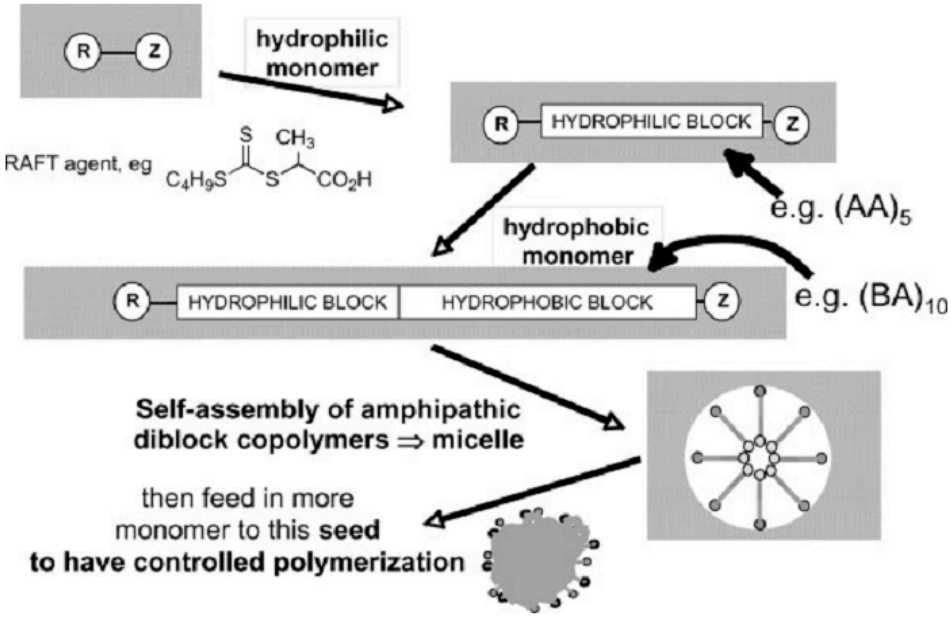

Scheme 2: MacroRAFT agent to produce core-shell polymeric structure [20].

With a similar principle, the group of Charleux [10, 17, 21] developed a method using a macroRAFT agent which based on poly (ethylene oxide) (PEO) as the hydrophilic moiety. In their study, another trithiocarbonate RAFT agent (2-(docdecylthiocarbonothioylthio)-2-methyl propanoic acid (TTC-A) was used to create an amphiphilic PEO macroRAFT agent by attaching the hydrophilic PEO chain to the carboxylic acid group of TTC-A via an esterification reaction. The newly formed PEO macroRAFT exhibited a structure close to a classical nonionic surfactant which is suitable to perform polymerization with various monomers. The process is presented in Scheme 3.

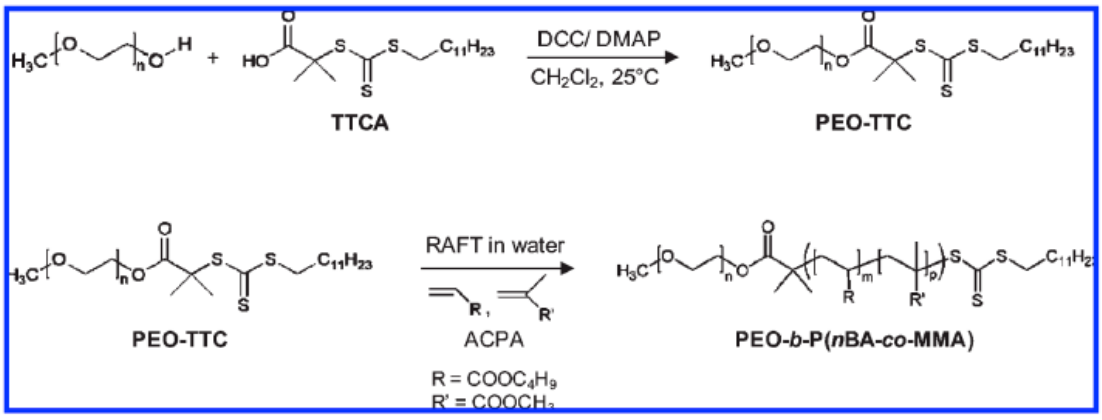

Scheme 3: Preparation of PEO-macroRAFT agent and copolymerization with butyl acrylate and methyl methacrylate [17].

In a recent work, Boisse et al. [22] reported a method using a macroRAFT agent to prepare copolymers with different morphologies such as nanospherical or filamentous by changing the pH or the composition of macroRAFT agent. The macromolecular RAFT agent used in the study was composed of acrylic acid and poly(ethylene glycol) methyl ether acrylate (PEGA) end-capped by TTC. By varying the relative hydrophilic proportion and the reaction conditions, styrene was polymerized in aqueous conditions with various morphologies and sizes. Scheme 4 presents the synthetic approach of the team.

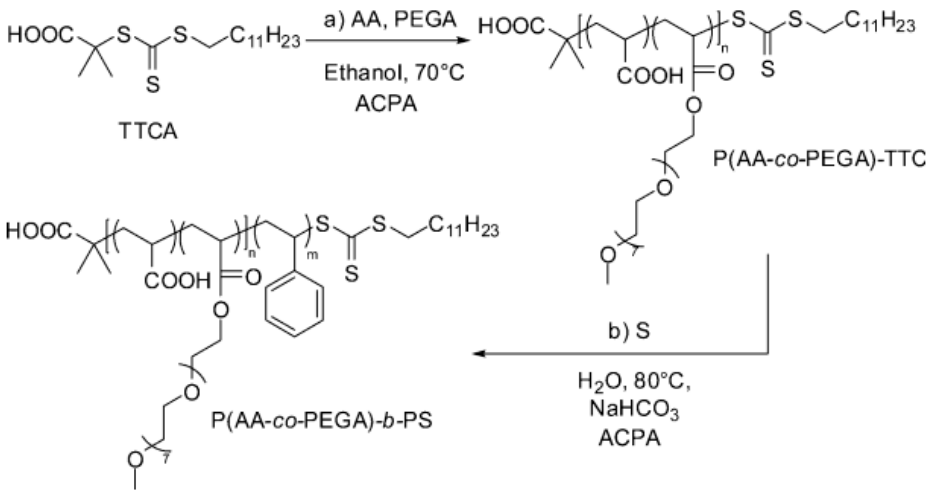

Scheme 4: Synthetic approach to prepare macroRAFT agent and polymerization of styrene [22].

1.2.3. RAFT polymerization in emulsion

There are many advantages in carrying out polymerization in water instead of in solution or bulk that are the environmental friendly reaction medium, the highly efficient heat transfer and the ability to control the morphology as well as the conversion of the polymerization.

The polymers formed using emulsion polymerization techniques are called latexes which can vary in chemical composition and particle morphologies namely core-shell, hemisphere, salami, raspberry or separated individual particle [11]. There are various systems to implement heterogeneous polymerization, among which, two main ones which are suitable for RAFT polymerization are discussed next.

1.2.4. Ab initio emulsion polymerization

An ab initio emulsion system contains a water-soluble initiator, water-insoluble vinyl monomer, a surfactant and water. While mixed together, those ingredients form monomer – swollen micelles dispersed in water along with large droplets of monomer which are stabilized by the surfactant. Upon heating, the initiator decomposes and triggers the polymerization. The monomer in the water phase will first react with the radicals until they reach a critical chain length which is above their solubility in water. In the following step, the growing oligomer enters the micelles which have a monomer – rich environment. The growing oligomers inside the micelles propagate rapidly to form the latex. Diffusion of monomer from non-nucleated micelles and monomer droplets will occur to feed the polymerization growing inside the nucleated micelles. By using RAFT along with macro-RAFT agents which can also act as surfactant, one can commence ab initio emulsion to prepare block copolymers. Stoffelback et al. [10] used a surface-active RAFT agent, the 2-(dodecylthiocarbonothioylthio)-2-methylpropanoic acid (TTC-A) as both chain transfer agent and emulsifier to perform surfactant free ab inito emulsion polymerization of n-butyl methacrylate and styrene. Wi et al. [23] reported the use of poly(methacrylic acid) as the macroRAFT agent which acted as both emulsifier and precursor to perform a “soap free” emulsion polymerization of styrene.

1.2.5. Miniemulsion Polymerization

Different from ab initio emulsion polymerization, in miniemulsion there is a cosurfactant which helps stabilizing the monomer droplets whose diameter can vary between 50 nm and 500 nm. The role of cosurfactant is very important since it prevents the diffusion of monomer between droplets or the coagulation of droplets. Miniemulsion polymerization with utilization of RAFT techniques has been also applied to prepare novel polymer systems [7, 24]. However, miniemulsion polymerization requires more drastic conditions such as the use of a high-sheering process ultrasonication, thus restrict its application.

1.3. Nanocomposite preparation methods using RAFT method.

The RAFT technique polymer/inorganic nanocomposite materials can be prepared following four main methodologies:

1. In situ preparation in which the inorganic precursors are mixed with polymer and the synthesis of nanoparticles is performed in the presence of the polymer;

2. Surface initiating polymerization or “grafting from”: the chain transfer agent is grafted to the surface of the nanoparticles. From which, polymerization is carried out to form nanocomposites;
3. Grafting through methods: the inorganic particles are modified with polymerizable moieties. The polymerization is carried out through these moieties to form nanocomposite.[25]
4. “Grafting to”: polymer and nanoparticles are mixed to yield covalent bonding within the nanocomposites.
5. Blending: polymer and nanoparticles undergo physical adsorption to form nanocomposites

Scheme 5 demonstrates the above discussed methods where blending and the grafting to approach are considered the same.

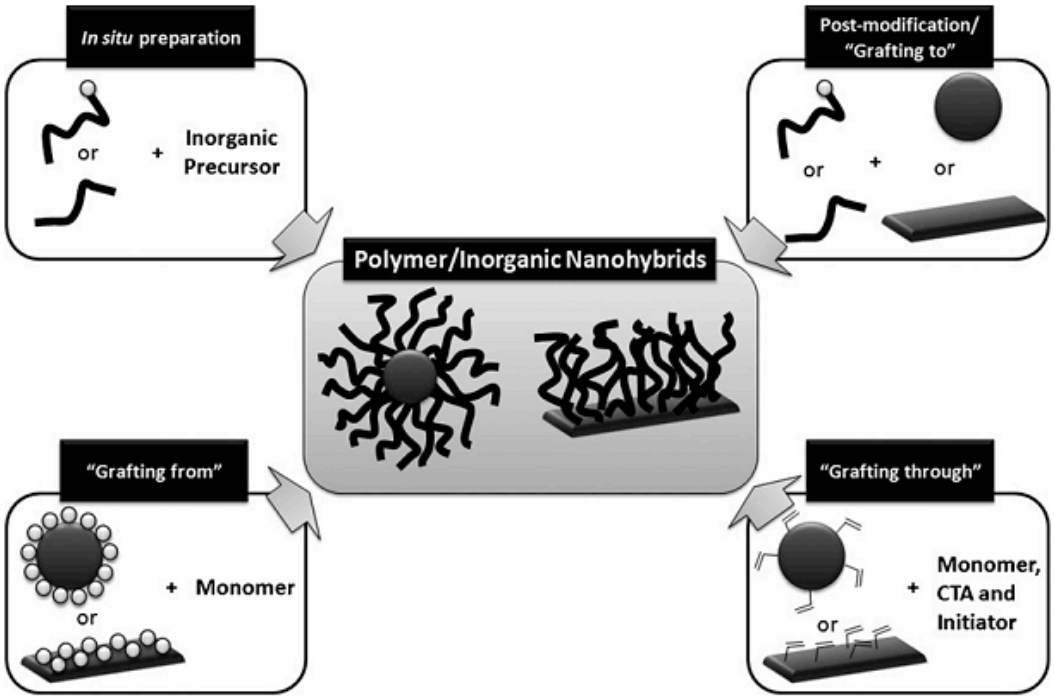

Scheme 5: Common methodologies to prepare polymer/inorganic nanocomposite materials [25]

1.3.1. Grafting to

In this method, the polymers which were pre-synthesized by RAFT contain dithioester or trithiocarbonate end groups, which can be reduced to thiol groups with the help of $NaBH_4$. The surface of inorganic particles which has high affinity for thiol groups will form covalent linkage with the polymer through the functional groups. Scheme 6 shows the mechanism of the process.

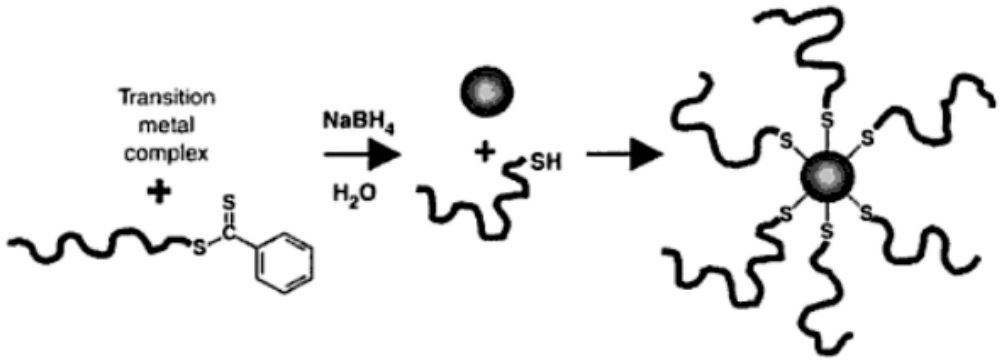

\

Scheme 6: “Grafting to” method mechanism[3]

There are limitations associated to this approach such as the difficulty of diffusion of polymers into the surface which reduces the density of the surface grafting. The thiol-metal bonding also restricts the application of the approach only to metal particles.

1.3.2. Grafting from

To overcome the diffusion of the polymer to the target particle associated with the “grafting to” technique, “grafting from” strategy is considered to be a promising alternative. In this method, the RAFT agents are anchored to the surface of the particle through covalent bonding. Growing from the surface polymerization is commenced afterwards under living radical conditions. There are two ways to graft the RAFT agent onto the surface of particle which are through the R group or the Z group approach.

In R-group grafting, the surface is attached with the leaving R group, thus, the solid particle acts as a leav*i*ng part containing radicals. The propagation happens on the surface. Li et al. [6] grafted the RAFT agent on the surface of nano size silica through various chemical steps. Scheme 7 shows the work of those authors.

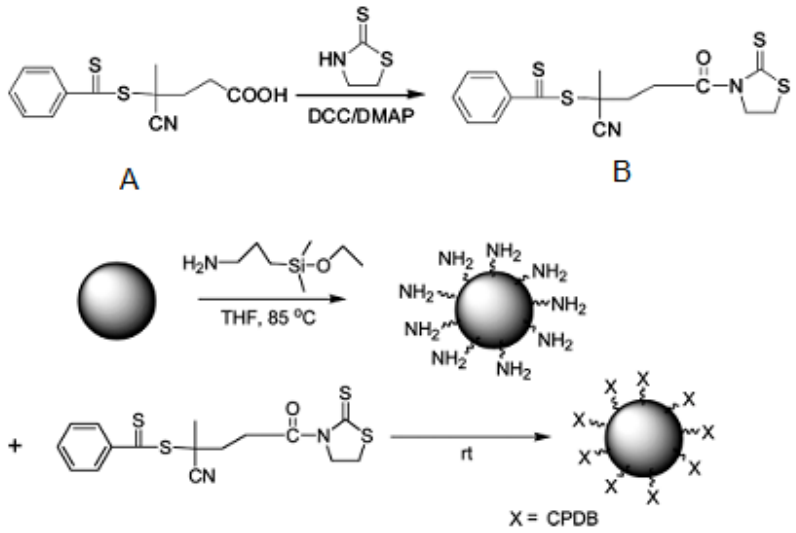

Scheme 7: Synthesis Procedure of 4-Cyanopentanoic Acid Dithiobenzoate onto Silica Nanoparticles [6]

In this work, the R group of the RAFT agent A was activated before reacting with the amino groups on the surface of silica which had been previously treated with suitable agents. In deed this method will be discussed later in 1.4.2. The modified surface was then involved in living polymerization using various monomers such as MMA and styrene.

Another approach was conducted by Jiliang Liu et al [26] using *in situ* synthesize RAFT agent on the surface of phenyl methyl chloride-modified Silica surface. 4- vinyl pyridine was used as monomer in the RAFT polymerization to form the shell layer covering the silica particle. Au nanoparticles are also embedded in the polymer shell to create a hybrid nanocomposite. Scheme 8 shows how the works were done.

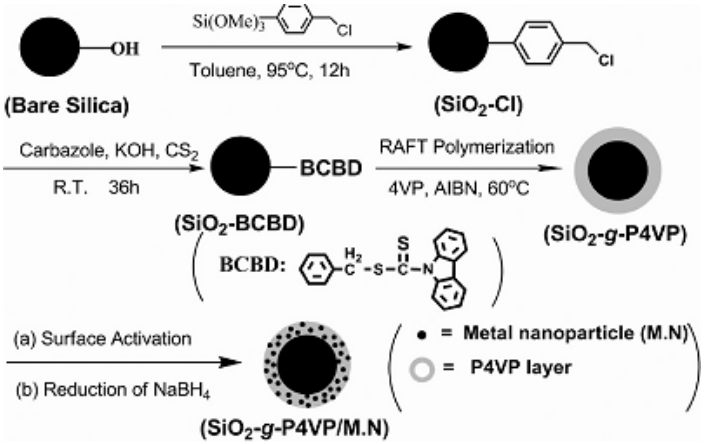

Scheme 8: Grafting from using RAFT on the Silica [26]

Barros et al. [27] also employed the “grafting from” method to prepare quantum dots/polymer nanocomposite by RAFT polymerization in miniemulsion. The CdS quantum dots surface was functionalized using a RAFT chain transfer agent - a trisalkylphosphine oxide incorporating 4-cyano-4-(thiobenzoylsulfanyl)pentanoic acid moieties . The RAFT process to graft poly styrene on the surface of the quantum dots was activated using a free radical initiator AIBN.

In Z-group grafting, the surface of the particles is anchored with the RAFT agent through the stabilizing group. The RAFT agent is permanently attached to the surface while the leaving group R propagates in the medium before reattaching with the surface. This approach is to some degree similar to the “grafting to” method. Therefore, this approach faces the same hindrance as the “grafting to” method due to the steric hampering on the surface, resulting in a limited number of researches utilizing this approach.

More recently, MacroRAFT agents have also been used in the preparation of nanocomposite materials in aqueous media. Ali et al. [12] used a macroRAFT agent containing a random copolymer of acrylic acid and butyl acrylate to stabilize the clay gibbsite without using an external surfactant. The latter encapsulation by MMA was done using a macroRAFT agent containing copolymer BA_5-co-AA_{10}. Anisotropic latex particles were achieved with good platelet orientation. In another work, Daigle et al. [28]reported a simple method to prepare nanocomposite of various inorganic nanoparticles. The authors prepared a macroRAFT agent comprising of poly(acrylic acid) and disperse the homopolymer into the dispersion of inorganic nanoparticles in water. Next, the copolymerization between Buty acrylate and acrylic acid was commenced on the surface of the nanoparticles yielding hybrid materials. The approach offers the possibility to be applied to a variety of metal oxides (alumina, rutile, anatase, barium titanate, zirconia, copper oxide), metals (Mo, Zn), and even inorganic nitrides (Si_3N_4).

1.4. Nanofillers preparation

Significant interests have emerged in the synthesis of nanoscale materials due to their different or enhanced properties over bulk materials. In this work, attention will be paid to two families of nano-sized fillers which are spherical silica nanoparticles and ZnO nanowires.

1.4.1. ZnO nanowires preparation

One of the interesting classes of semiconductor materials is semiconductor oxides. Out of these oxides, zinc oxide is of particular interest due to their application as building blocks in the fabrication of nanodevices due to its abundance, nontoxic nature, excellent electrical conductivity, high optical transparency in the visible wavelength region, and good chemical stability in reducing environments. Moreover, zinc oxide has a direct wide band gap (3.37 eV) and high exciton binding energy (60meV) at room temperature.

One-dimensional (1-D) zinc oxide nanostructures have received increasing attention in comparison to the bulk material because of their novel and unique properties which have opened a wide range of applications. Among them ZnO nanowires possesses a very high surface-to-volume ratio characteristic is promising as building block for fabricating nanodevices. Therefore, zinc oxide nanowires have been studied and synthesized widely by various processes.

Synthetic methods of ZnO nanowires

Various methods to produce ZnO nanowires, such as pulse laser deposition (DLP), metal-organic vapour deposition (MOCVD), molecular beam epitaxy (MBE), sol-gel method and hydrothermal method have been widely investigated. These methods can be divided into two main groups: physical and chemical methods.

Physical methods

In physical methods, Zn and O elements are let to react with each other in the vapour phase and the products condense onto a substrate. There are several ways to transform Zn into vapour phase. Elevating temperature and pulsed laser deposition are among the common means to achieve Zn vapour from the precursor.

Gangmeng et al. [29] investigated the influence of the gas carrier and the deposition position on the length of growth ZnO nanowire grown by the vapour phase method. The setup and the resultant ZnO nanowire are shown in Figure 4

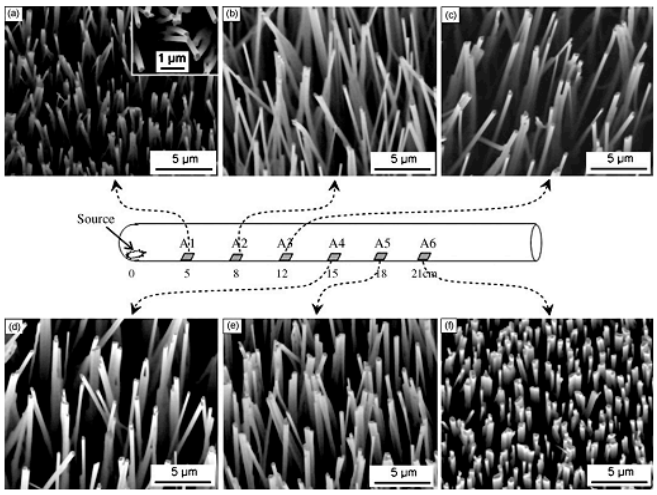

Figure 4: ZnO nanowires grown by vapor transport method [29] in which A(1-6) are the substrates placed at different distances from the source.

Electrochemical deposition methods

In order to lower the working temperature and harsh conditions of ZnO nanowire synthesis required by the vapour transport method, electrochemical deposition has the advantage to work at relatively low temperature. The main reaction is the reduction of dissolved molecular oxygen in Zn^{2+} solution. Close to the cathode, oxygen is reduced to form OH- ions. The formation of hydroxide ions increases the pH value at the cathode and as a result Zn^{2+} and OH^{-} react with each other to form ZnO which precipitates and deposits on the surface of cathode. The growth of ZnO nanowires can be carried out either on a seeded layer of ZnO or on a membrane template.

Chemical methods

To overcome the complexity of equipment and rigorous conditions of other methods, the hydrothermal method has been proposed as a low temperature synthesis technique (90-250^{o}C). The method has been developed for large scale low temperature production of ZnO nanowires. In the hydrothermal method ZnO nanowires can be grown either on a substrate or without a substrate. The advantage of the hydrothermal method is the variety of substrates that can be used and which is usually limited in other methods due to the harsh conditions. Substrates used for nanowire growth can be glass, silicon, or even plastic.

Another simple approach to synthesize ZnO nanowires was conducted by Lin et al. [30]. In their work, a free- catalyst thermal decomposition of Zinc acetate dihydrate as the precursor was conducted to produce high purity single crystal ZnO nanowires. The reaction was performed at 300^{o}C in an alumina crucible. ZnO nanowires were collected on the wall and the lid of the crucible. The mechanism of the decomposition and crystallization process was studied by various characterization techniques such as TGA, GSC and MS. The product was characterized by X-Ray diffraction, TEM and SEM which indicated the fabrication of single crystalline, large aspect ratio ZnO nanowires.

1.4.2. Silica nanoparticles preparation

The simplest and the most used method to prepare silica nanoparticles was reported by Stöber et al. [31]. In that method, the author made used of a sol-gel process which is based on the hydrolysis of a dilute solution of tetraethylorthosilicate (TEOS) in ethanol at high pH. The hydrolysis was then followed by condensation which yielded silica spheres. The hydrolysis and condensation reactions of TEOS are shown in

Scheme 9

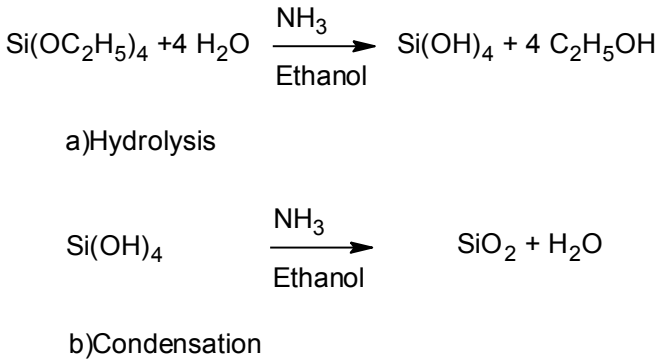

Scheme 9: a) Hydrolysis of TEOS and b) Condensation process to yield Silica nanospheres.

By changing the concentration of the reactants, the authors were able to achieve uniform amorphous spheres with varying sizes from 10 nm to 2 μm. Many others have also studied and improved the Stöber method [32-34]. Due to those studies, it is now established that the diameter and the size distribution depend strongly on the reaction conditions such as reactants concentration ratios, type of solvent and temperature.

To control the particle morphology, templates have also been used such as micelles and microemulsion [35, 36] [37] using surfactants including cationic, anionic and nonionic.

Silica surface modification

Naturally, the surface of silica nanoparticles possesses a negative charge due to the ionization of the hydroxyl groups on the surface. These hydroxyl groups act as stabilizations groups to prevent aggregation but can be modified with a variety of silanes to tune the surface properties of SiO_2 NPs in order to promote compatibility with the polymer matrix. Functional groups such as amide, epoxy, and acrylate etc. can be anchored to the surface via suitable procedures.

Modification procedure

A common strategy to modify the surface of silica nanoparticles prepared using the Stöber method is to use organoalkoxysilane compounds. Under acid-base chemical environment, the silane coupling agents undergo hydrolysis and condensation processes, resulting in the anchoring of functional group onto the surface of silica. Figure 5 presents the general strategy to modify silica nanoparticles.

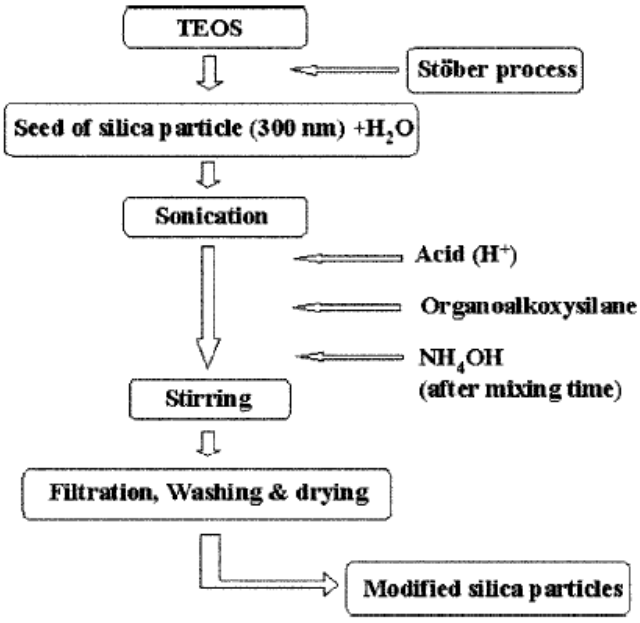

Figure 5: Chart of two-step process for silica modification [38]

The organoalkoxysilane compounds used in the process contain two types of reactive functional groups. One group is hydrolysable while the other is non- hydrolysable.

There are two steps reactions: hydrolysis and condensation

1) Hydrolysis:

$$XSi(OR)_3 + nH_2O \rightarrow XSi(OR)_{3-n}(OH)_n + nROH$$

2) Condensation can occur between OH group and silanol groups on the surface of silica as shown in Figure 6 or self-condensation of hydrolyzed silane molecules as shown in Figure 7. The latter is undesired.

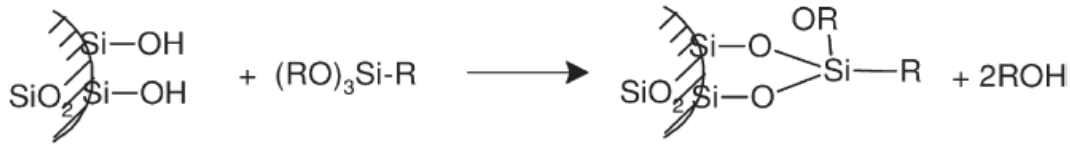

Figure 6: Reaction between silanol group and trialkoxysilanes [39]

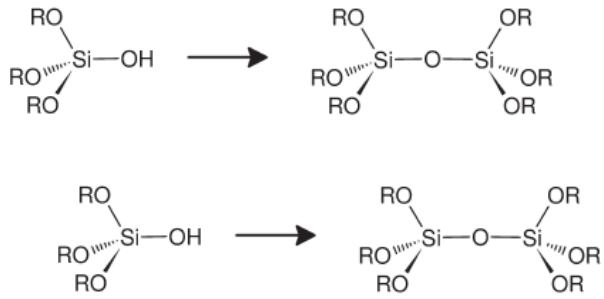

Figure 7: Self condensation of trialkoxysilanes [39]

Two of the most common silane coupling agents are 3-(trimethoxysilyl)propyl methacrylate (MPS) and 3-aminopropyltrimethoxysilane (APS).

Following the mechanism discussed above in Figure 6 and Figure 7, Bourgeat Lami et al. [39] used MPS as organophilic agent to coat silica alcosol particle surface. The coating was achieved by stirring a mixture of alcosol and MPS for several days at room temperature and pH was kept constant at near natural to prevent homocondensation of MPS. Excessive MPS was used: 40 µmol of coupling agent per square meter of silica, corresponding to five times the silanol surface concentration which is approximately 8 µmol/m^2. Free MPS after reaction were separated by dialysis.

On the other hand, the modification with APS undergoes a different mechanism. T. Jesionowski et al. [40] explained the condensation step between aminosilane and

silanol as shown in Figure 8. At first, the amine groups establish H-bonds with the silanol groups on the surface of silica. Then, a condensation reaction between the silane moiety of the APS and the adjacent silanol moiety of the silica occurs, causing a flip of the APS molecules. In the final stage, the amine group has an up-position which behaves as a functional group on the silica nanoparticles available to participate in the formation of nanocomposites.

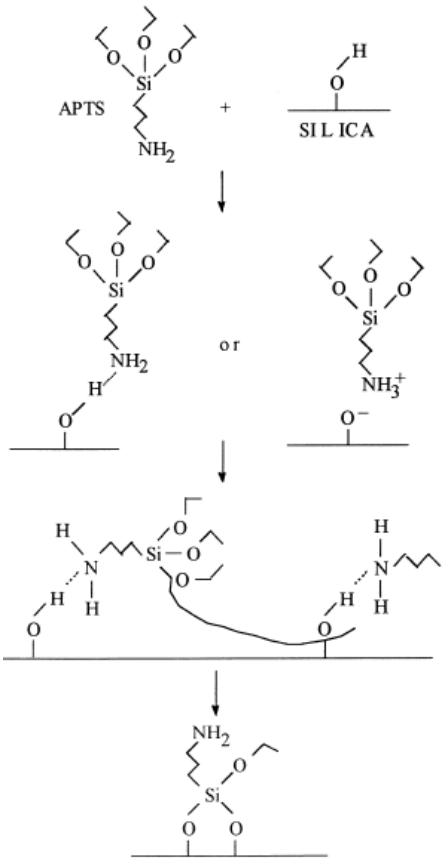

Figure 8: Mechanism of grafting a typical aminosilane to a silica surface [40]

By modifying silica with organoalkosilane groups such as 3-(trimethoxysilyl) propylmethacrylate (MPS) or 3-aminopropyltrimethoxysilane (APS), the functional groups: double bond with MPS and amino group with APS are anchored onto the surface. In nanocomposite preparation, these groups promote the affinity between the nanoparticles and the polymer matrix. Furthermore, they can also be used to anchor the RAFT agent which is used to conduct the living radical polymerization via the “grafting from” approach discussed in 1.3.2.

1.5. Objectives of the Thesis

Polymer/ Inorganic nanomaterials are very promising in many advanced applications due to their unique properties. However, preparation methods of these materials have been facing many obstacles. Especially, “green methods” which replace hazardous organic solvents by water still have many drawbacks such as colloidal instability and poor control over polymerization. Therefore, the objectives of this thesis are:

- To understand the state of art of preparation methods of polymer/inorganic nanomaterials.
- To produce, modify and characterize nano inorganic particles (Silica spherical nanoparticles and ZnO nanowires)
- To understand and apply RAFT polymerization to prepare macroRAFT agents using acrylic acid and poly (ethylene glycol) methyl ether acrylate.
- To perform emulsion polymerization using macroRAFT agents to prepare and characterize copolymers of acrylic acid or poly(ethylene glycol) methyl ether acrylate with butyl acrylate
- To perform emulsion polymerization using macroRAFT agents to prepare nanocomposites based on block copolymers and Silica nanoparticles or ZnO nanowires.

2. EXPERIMENT

2.1. Instruments

- Proton NMR Broker Avance/300; Frequency 300 MHz; Solvents: $CDCl_3$, D_2O, DMSO were used to measure Proton-NMR
- Scanning Electron Microscopy (SEM) FEG-SEM Hitachi S4100 field emission microscope was used to take SEM images
- Malvern zeta-potential analyzer was used to measure particle size and zeta potential
- Dynamic Mechanical Analysis (DMA) was perform using a Tritec 2000 from Triton Technologies
- Gel Permeation Chromatography (GPC) spectra was recorded using a PL-110GPC
- Attenuated Total Reflection Fourier Transformed Infrared Spectra (ATR-FTIR) were recorded on a Matson 7000 FTIR spectrometer in absorbance mode
- Water was purified using a Sation 8000/ Sation 9000 purification unit

2.2. Materials

Zinc acetate -2-hydrate (99%,Riedel-de Haen); acrylic acid (99%, Sigma Aldrich); butyl acrylate (99%, Sigma Aldrich), poly(ethylene glycol) methyl ether acrylate (Mn=480 g/mol, Sigma Aldrich); methyl methacrylate (Sigma Aldrich); TTC-A (2-(docdecylthiocarbonothioylthio)-2-methyl propanoic acid (synthesized by Barros Timmons and Charleux),; N,N-dimethyformamide ACS reagent (99%, Sigma Aldrich); ethanol (99.9%Fluka), chloroform (99%, Sigma Aldrich). Initiator used in the polymerization reactions was 2,2'- Azobis (2-methylpropionamidine) dihydrochloride (97%, Sigma Aldrich)

Acrylic acid, butyl acrylate and methyl methacrylate were purified by passing through alumina column.

2.3. Procedures

Zinc Oxide nanowire Preparation

ZnO nanowire was prepared following the procedure reported by Lin et al. [30]. Zinc acetate dehydrate (0.5g) was put into an alumina crucible with a lid which was then placed inside an oven. The oven was heated to 300 ^{o}C for 15 hours. Heating rate was

kept at 10 Celsius degree/minute and cooling rate at 5 Celsius degree/minute. The product was collected from the wall of the crucible and on the lid and was characterized by FTIR, X-ray diffraction and SEM.

Polymerization procedure

Polymer preparation procedures were adapted from the work of Ferguson et al. [19] and the group of Charleux [22] with minor adjustments.

Synthesis of PAA_6-TTC macroRAFT agent

In a typical procedure, Acrylic acid (0.32 g, 0.0044 mol), TTC-A (0.27g, 0.00074 mol) and DMF (15 mL) were transferred into a 25 mL round bottom flask and the mixture was stirred until complete dissolution of TTC-A was observed. Initiator (0.0169 g, 0.000078mol) was added and the mixture was degassed under Nitrogen flow for 30 minutes in an ice bath under stirring. The reaction was performed at 80 ^{o}C for 100 minutes under constant stirring. The reaction was terminated by immersing the flask into an ice bath along with exposing the reaction mixture to air. The sample was precipitated from n-hexane with the ratio of n-hexane/reaction solution =10 to remove unreacted monomer and DMF. In order to remove residual of DMF, dialysis against water was performed. Lyophilization was conducted to dry the sample. The product was characterized with FTIR, ^{1}H-NMR and GPC.

PAA_{60}TTC macroRAFT agent was taken from the work of Carvalho [41] and repurified from n-hexane without performing dialysis and lyophilization.

Synthesis of Copoly (Acrylic acid-co-Butyl acrylate)

In a typical procedure, the copolymerization was done in emulsion. PAA_{60}TTC (0.12 g) was dissolved in H_2O (3 mL) in a 5 mL round bottom flask. $NaHCO_3$ (0.07 g) was dissolved in water (0.5 mL) which was then added to the flask to adjust pH at 8. Initiator (0.001 g) was dissolved in of H_2O (0.5 mL) and added to the round bottom flask. Butyl Acrylate (0.53 mL (0.48 gram)) was added to the mixture. The mixture was immersed in an ice bath and degassed by Nitrogen flow for 30 minutes in an ice bath under stirring. The contents were allowed to react at 70^{o}C for 4 hours. After the reaction, the mixture was immersed in an ice bath and exposed to air. 1 mL of the emulsion was withdrawn to make a film on an aluminum dish. After normal evaporation during night, the film was dried overnight at 60 ^{o}C until constant weight in a ventilated oven. Part of the film was

characterized by DMA and the remaining was used to prepare solutions for ^{1}H-NMR, FTIR and GPC analyses. The emulsion was characterized by DLS.

Preparation of nanocomposite

Preparation of Silica@APS nanocomposite

PAA_{60}TTC (0.12 gram) was dissolved in H_2O (3 mL) in a 5 mL round bottom flask. $NaHCO_3$ (0.07g) was dissolved in water (0.5 mL) which was then added to the flask to adjust pH to 8. SiO_2@APS (0.03 g) equal to 5%wt towards the mass of polymer was added into the solution. The mixture was stirred and sonicated in 30 minutes. Initiator (0.0017 g) was dissolved in H_2O (0.5 mL) and added to the round bottom flask. Finally, Butyl Acrylate (0.53 mL) was added and the mixture was degassed under Nitrogen flow for 30 minutes in an ice bath under stirring. The contents were allowed to react at 70^{o}C for 4 hours. After the reaction, the mixture was immersed in an ice bath and exposed to air. 1 mL of the emulsion was withdrawn to make a film on an aluminum dish. After normal evaporation during night, the film was dried overnight at 60 ^{o}C until constant weight in a ventilated oven. Part of the film was characterized by DMA and the remaining was used to prepare solutions for FT-IR and GPC analyses. The emulsion was characterized by DLS and SEM.

Synthesis of P(PEGA)-TTC macroRAFT agent- MacroRAFT 3

Following the procedure of Boisse et al. [22], TTC-A (0.161 g, 0.00044 mol) were mixed in 5.1 mL of ethanol until complete dissolution. Initiator (0.0082g, 3.10^{-5} mol) and PEGA (9.2 g, 0.0191 mol) were added consequently and the mixture was degassed under Nitrogen for 30 minutes in an ice bath under stirring. The reaction was carried out in 70 ^{o}C for 4 hours. The reaction was terminated by exposing to air and cooling down using an ice bath. The polymer was recovered from cold diethyl ether to remove all unreacted monomerand residual ethanol. The polymer was then dried under reduced pressure at 50 ^{o}C over night. The polymer was characterized by GPC, ^{1}H-NMR and FTIR.

Synthesis of P(PEGA)-TTC-co- butyl acrylate (Coplymer4)

P(PEGA)-TTC macroRAFT agent (0.52 g) was dissolved in 2.5 mL of ultra pure water. . A stock solution (1 mL) of initiator (3.2 mM) containing $NaHCO_3$ (10mM) to help dissolution, was added to the mixture. The monomer, Butyl acrylate (0.61 mL) was added and the mixture was degassed under Nitrogen for 30 minutes in an ice bath under stirring. The reaction was carried out in 70 ^{o}C for 4 hours. The reaction was

terminated by exposing the mixture to air and cooling down using an ice bath. 1 mL of the emulsion was withdrawn to make a film on an aluminum dish. After normal evaporation during night, the film was dried overnight at 60 ^{o}C until constant weight in a ventilated oven. Part of the film was characterized by DMA and the remaining was used to prepare solutions for ^{1}H-NMR and GPC analyses. The emulsion was characterized by DLS.

Synthesis of P(PEGA)-TTC-co- methyl methacrylate (MMA)-Copolymer5

The copolymerization process was similar to copolymerization with butyl acrylate. Butyl acrylate was replaced by MMA. The molar ratio of MMA and macroRAFT agent was 147.

Nanocomposite preparation using P(PEGA)-TTC as macroRAFT agent –Sicom 4

Silica modified by APS was used as filler in nanocomposite preparation. Silica@APS was used with 5% in weight relative to initial monomer and macroRAFT agent mass. Firstly, P(PEGA)-TTC macroRAFT agent (0.52 gram) was dissolved in ultra pure water (2.5 mL). Silica@APS (40 mg) was added into the solution. The mixture was then sonicated in 30 minutes to ensure the dispersion of Silica. . A stock solution (1 mL) of initiator (3.2 mM) containing $NaHCO_3$ (10mM) to help dissolution, was added to the mixture. The monomer, Butyl acrylate (0.61 mL) was finally added and the mixture was degassed under Nitrogen for 30 minutes in an ice bath under stirring. The polymerization was conducted at 70 ^{o}C for 4 hours. The polymerization was quenched by immersing the mixture in an ice bath and exposing the mixture to air. 1 mL of the emulsion was withdrawn to make a film on an aluminum dish. After normal evaporation for one night, the film was dried overnight at 60 ^{o}C until constant weight in a ventilated oven. Part of the film was characterized by DMA and the remaining was used to prepare solutions for FT-IR analyses. The emulsion was characterized by DLS and SEM.

Synthesis of P(AA-PEGA)-TTC macroRAFT agent-MacroRAFT 4

TTC-A (0.161 g) were mixed in 5.1 mL of ethanol until complete dissolution. Initiator (0.0082 g) and PEGA (4.5mL) and Acrylic acid (0.68mL) were added consequently under Nitrogen in 30 minutes in an ice bath under stirring. The reaction was carried out in 70 ^{o}C for 55 minutes. Upon which the reaction was terminated by exposing to air and cooled down in an ice bath. The polymer was recovered in cold diethyl ether to remove all unreacted monomer. The polymer was then dried under reduced pressure at 50^{o}C over night. The polymer was characterized by DMA, GPC, ^{1}H-NMR, FTIR.

Synthesis of copolymer P(AA-PEGA-BA)-Copolymer6

P(AA-PEGA)-TTC macroRAFT agent (0.52 gram) was dissolved in 2.5 mL of ultra pure water. . A stock solution (1 mL) of initiator (3.2 mM) containing $NaHCO_3$ (10mM) to help dissolution, was added to the mixture. The monomer, Butyl acrylate (0.61 mL) was finally added and the mixture was degassed under Nitrogen for 30 minutes in an ice bath under stirring. The polymerization was conducted in an oil bath thermostated at 70 ^oC for 4 hours. The polymerization was quenched by immersing the mixture in an ice bath and exposing the mixture to air. 1 mL of the emulsion was withdrawn to make a film on an aluminum dish. After normal evaporation for one night, the film was dried overnight at 60 ^oC until constant weight in a ventilated oven. Part of the film was characterized by DMA and the remaining was used to prepare solutions for ^1H-NMR and GPC analyses. The emulsion was characterized by DLS.

Preparation of Nanocomposite of Silica and copolymer 6 (Sicom 6)

Firstly, P(PEGA)-TTC macroRAFT agent (0.311 gram) was dissolved in 2.5 mL of ultra pure water. Silica@APS (40 mg) was added into the solution. The mixture was then sonicated in 30 minutes to ensure the dispersion of silica. A stock solution (1 mL) of initiator (3.2 mM) containing $NaHCO_3$ (10mM) to help dissolution, was added to the mixture. The monomer, Butyl acrylate (0.52 mL) was finally added and the mixture was degassed under Nitrogen for 30 minutes in an ice bath under stirring. The polymerization was conducted in an oil bath thermostated at 70^oC for 4 hours. The polymerization was quenched by immersing the mixture in an ice bath and exposing the mixture to air. 1 mL of the emulsion was withdrawn to make a film on an aluminum dish. After normal evaporation for one night, the film was dried overnight at 60 ^oC until constant weight in a ventilated oven. After drying, a part of film was characterized by DMA, ATR-FTIR. The emulsion was characterized with SEM and DLS.

Methylation Process

For Gel Permeation Chromatography, the polymers were modified by methylation of the carboxylic group using trimethylsilyldiazomethane. The process was based on a published protocol [42]. The homopolymers and the copolymers were first dissolved in a THF/methanol mixture (9:1). 50 mg of each sample was dissolved in 10 mL of solvent mixture. The yellow solution of trimethylsilyldiazomethane was added dropwise to the polymer solution. Upon addition, bubbles appeared. The addition was continued until the solution stopped bubbling. The solution was then dried under nitrogen flow to

remove solvent. 10 mg of samples were dissolved in 1mL of THF and filtered through a 0,3 μm membrane prior to GPC analyses.

3. RESULTS AND DISCUSION

3.1. Poly(acrylic acid) macroRAFT agent system

Selection of RAFT agent

It has been found that for emulsion polymerization, the RAFT agent should be amphiphatic i.e. to have a hydrophobic part and another which is hydrophilic [14].This provides the ability to self-assemble to form micelles in water. The hydrophobicity of the RAFT agent can be achieved by choosing a proper hydrophobic Z group. The hydrophilic nature of the leaving R group can be improved with the addition of a hydrophilic polymer such as poly (acrylic acid) (PAA) or poly (ethylene oxide) (PEO).

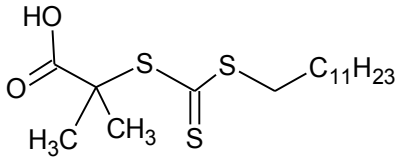

R: $-C(CH_3)_2COOH$

Z: $-SC_{11}H_{23}$

Figure 9: RAFT agent formula

The RAFT agent used in this study was 2-dodecylthiocarbonothioylthio)-2metyl propanoic acid (TTC-A). The structure is shown in Figure 9. This is a trithiocarbonate RAFT agent which shows high compatibility with many type of monomers and media, both aqueous and non-aqueous. Furthermore, trithiocarbonate RAFT agents also show high transfer constant over conventional dithioester compounds.

3.1.1. Preparation and characterization of PAA-TTC macroRAFT agents

Preparation of the macroRAFT agent

As discussed in the introduction there are two ways to form macroRAFT agents. The first way is to use TTC-A as a living chain transfer agent in the polymerization of acrylate monomers. This approach was used by Ferguson group [14, 18, 19] who produced macroRAFT agents with acrylic acid and TTC. The second approach is to use of the carboxylic end group of TTC-A to conduct an esterification process to attach a polymer chain into the RAFT agent. Charleux et al. have used this method to prepare PEO-TTC [10, 17, 21, 22]. In this study, the macroRAFT agent was synthesized

following the method reported by Ferguson group. Scheme 10 exhibits the preparation of the acrylic-acid based MacroRAFT agent.

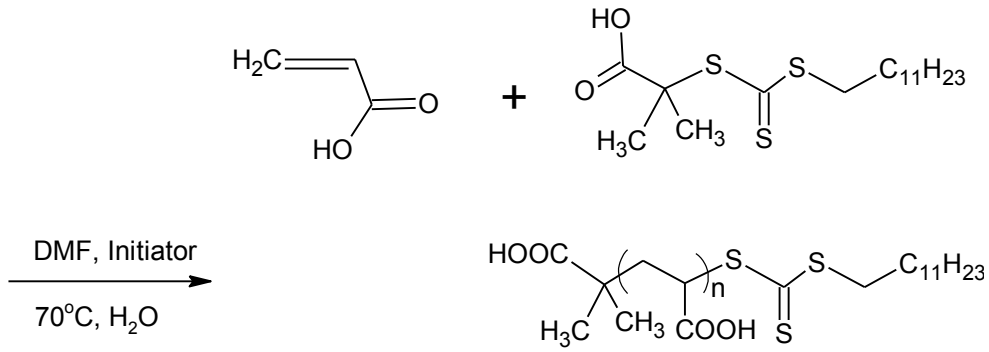

Scheme 10: Homopolymerization of acrylic acid using TTC-A as RAFT agent

The procedure was based on the study of Barros Timmons and Charleux [43]. In detail, the polymerization process was carried out at 70°C under nitrogen atmosphere for 100 minutes. After the reaction, the flask was plunged into an ice bath and exposed to air following the process described in 2.3.

In our study, two types of acrylic acid- based macroRAFT agent were prepared with two chain lengths of acrylic acid to study the effect of the hydrophilic part on the resulting copolymers. One macroRAFT agent was synthesized with expected 60 units of acrylic acid while another agent possessed a much shorter acrylic acid chain with expected 6 units.

The theoretical molecular weights were calculated following the equation:

$$M_{n,Theoretical} = \frac{[M]_0}{[RAFT]_0} x m_0 + M_{RAFT} \quad \text{equation (1)}$$

In which $[M]_0$ and $[RAFT]_0$ are the initial concentration of monomer and TTC-A respectively; x is the conversion and m_0 and M_{RAFT} are the molar mass of monomer and TTC respectively.

The short chain macroRAFT agent was used to prepare copolymers with butyl acrylate using two different concentrations of the reactants to test the stabilization ability of the macroRAFT agent. The list of macroRAFT agents and corresponding copolymers prepared is shown in Table 1.

Table 1: MacroRAFT agent preparation

MacroRAFT	[M]/[RAFT]	[RAFT] Mol/Litter solvent	[RAFT]/[I]	Time (minutes)	Temperature (^{o}C)
MacroRAFT 1 (PAA_{60}-TTC)	60	0.048	9	100	70
MacroRAFT 2 (PAA_{6}-TTC)	6	0.048	9	100	70

Characterization of the macroRAFT agent

The peaks at 1579 cm^{-1} and at 1735 cm^{-1} in the FT-IR spectra assigned to the C=O of the carboxylate groups and the C=O of the ester groups respectively indicate the presence of copolymers. See Annex 1 and 2.

^{1}H-NMR

The ^{1}H-NMR spectra of TTC-A and the MacroRAFT agent (PAA_{6}TTC) were taken after dissolving the samples in $CDCl_3$. The spectra are shown in Figure 10.

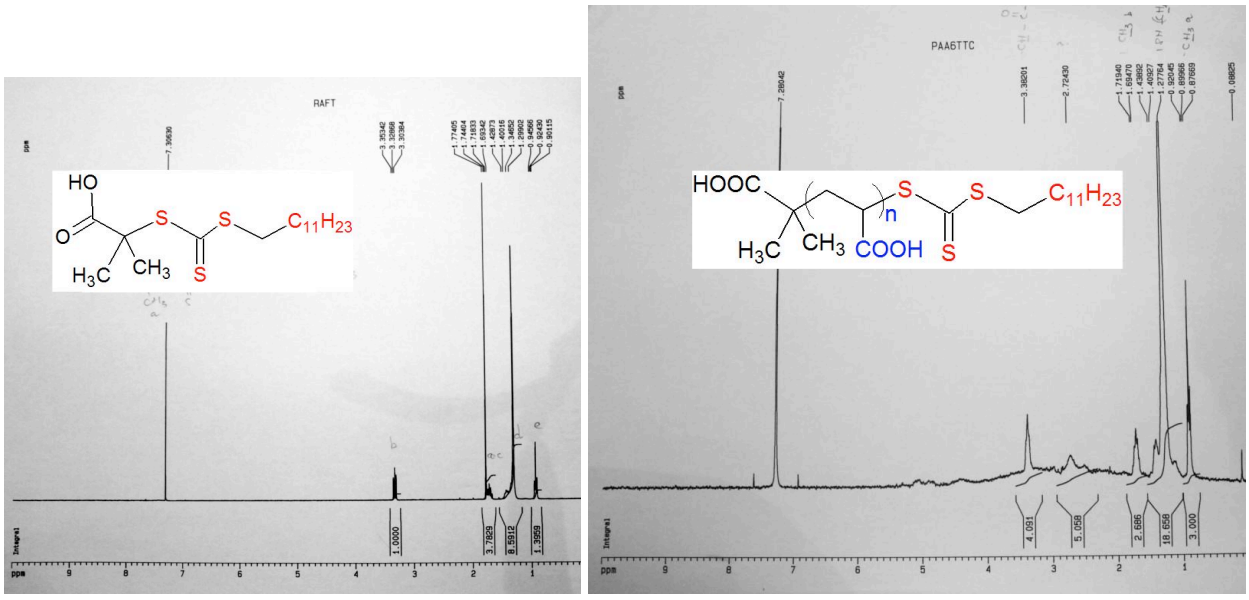

a b

Figure 10: ^{1}H-NMR spectra of TTC-A (a) and macroRAFT agent PAA_{6}TTC (b).

From Figure 10 a, characteristic peaks are found at 0.9 (t,3H, CH2CH3), 1.27(m,18H, -CH2(CH2)9CH3); 3.32 (t,S-CH2). In Figure 10 b the peaks of TTC were found confirming the presence of the RAFT agent moiety in the macromolecule. Furthermore, characteristic peaks corresponding to the presence of acrylic acid chain were found at 2.72 ppm and 1.71 ppm corresponding to Hα and Hβ respectively of acrylic acid units. The broadening of the peak at 1.27 which attributed to methylene proton also indicated the formation of polymer.

The ^{1}H-NMR spectrum of PAA_6TTC was also used to determine the degree of polymerization through the ratio between the integral of the characteristic peak of Hα of acrylic acid units at 2.72 ppm and the integral of the peak of $CH_3(CH_2)_9$ – at 0.87 ppm. Let n is the degree of the polymerization which is equal to the number of Hα proton. $I_{2.72}$ is the integral of the Hα peak and $I_{0.87}$ is the integral of the $CH_3(CH_2)_9$ peak, we have

$$I_{2.72}/n = I_{0.87}/3 \qquad \text{equation (2)}$$

From Figure 10b, we have $I_{2.72}$ =5.058 and $I_{0.87}$ = 3 giving n=5. Therefore, the degree of polymerization was 5.

3.1.2. Preparation and characterization of block copolymers

Preparation of Copolymer 1, 2 and 3

The process of copolymerization can be carried out in solution using ethanol as solvent or in water. The homogeneous reaction using organic solvent usually gives better results yielding stable solutions. In the case of using a heterogeneous systems, the main difficulty is to achieve colloidal stability of the system, along with good control of monomer conversion ensuring narrow molar mass distributions [19] . In our study, only emulsion polymerization was studied in order to improve the technique using water as an environmentally friendly medium and also to promote self assembly of the polymer chains during polymerization.

The block copolymers were prepared using PAA-TTC as the macroRAFT agent which acts both as the polymerization mediator and stabilizer without using any surfactant. Butyl acrylate was used as hydrophobic second as illustrated in Scheme 11 . In short, the macroRAFT agent was dissolved in water and $NaHCO_3$ was added to adjust the pH to 8. At high pH, the macroRAFT agent in water acts as a polyelectrolyte. The carboxylate groups possess negative charge which results in electrostactically repulsive force between those units. Scheme 11 shows the process of copolymerization.

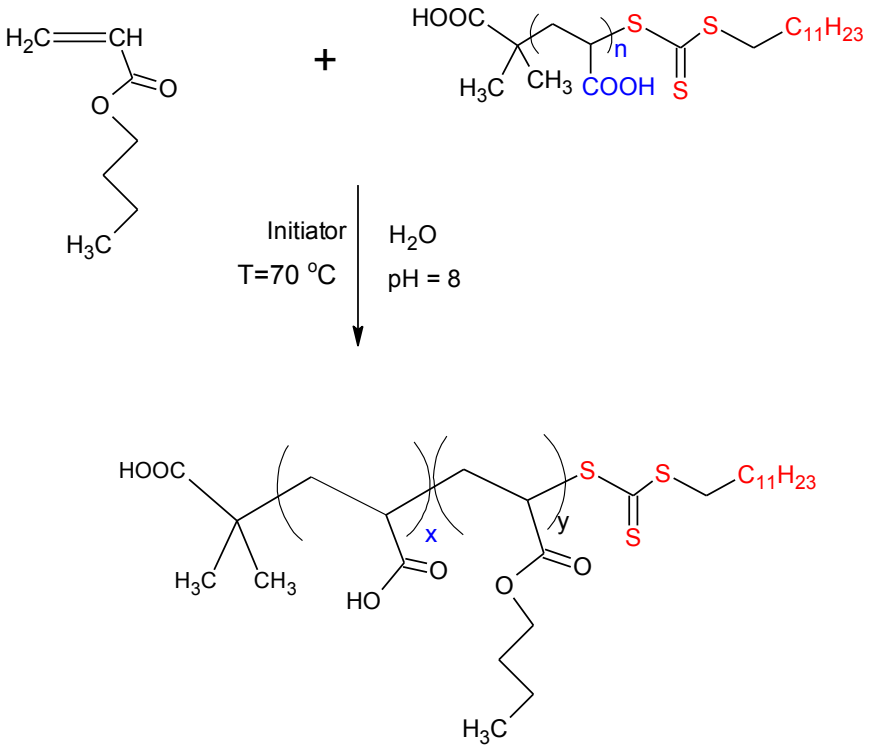

Scheme 11: Emulsion copolymerization of butyl acrylate and macroRAFT agent

Table 2 shows the list of copolymers prepared from the corresponding macroRAFT agents 1 and 2.

Table 2: Copolymers prepared from acrylic acid-macroRAFT agent

MacroRAFT	Copolymer with butyl acrylate	[M]/[RAFT]	[RAFT] Mol/Litter	[RAFT]/[I]	Time (hours)	Temperature (^{o}C)
MacroRAFT 1 (PAA_{60}-TTC)	Copolymer 1	147	0.0084	4	4	70
MacroRAFT2 (PAA_{6}-TTC)	Copolymer2	147	0.0084	4	4	70
	Copolymer3	147	0.0168	4	4	70

The role of the macroRAFT agent in emulsion polymerization can be described as following: the macroRAFT agents having a hydrophilic part and a hydrophobic part can act as a surfactant. In water, this macromolecular surfactant was used above the critical micelle concentration. Due to the amphiphilic nature of the agent, it assembled to form

micelles which have the hydrophobic part – the dodecyl pointing inward to be the core and the acrylic acid chain making up the shell. The micelle structure helped to stabilize the emulsion system. Upon addition of butyl acrylate, initiator and under proper temperature, ab initio emulsion copolymerization commenced. The process took place inside the preformed micelles thanks to the presence of the RAFT agent acting as a polymerization mediator.

Characterization of Copolymer 1, 2 and 3

After the reaction, 1 mL of emulsion was withdrawn to make a film on a tin dish. A part of the film was analyzed by DMA and the remaining was used to prepare solution for ^{1}H-NMR, FT-IR and GPC analyses. The emulsion was characterized by Dynamic light scattering (DLS).

^{1}H-NMR spectrum can be found in annex. The characteristic peaks assigned to TTC were found at 0.9 ppm (t,3H, $CH_2C\underline{H}_3$), 1.22 ppm (m,18H, $-CH_2(C\underline{H}_2)_9CH_3$); 3.32 ppm (t,S-$C\underline{H}_2$). Hα and Hβ of acrylic acid were found at 2.27 ppm and 1.27 ppm, ester methyl proton of butyl acrylate was found at 4.1 ppm, confirming the forming of the copolymer.

DLS results of the samples are presented in Table 3.

Table 3: DLS results of the PAA-BuA copolymers

Samples	Peak 1(nm)	Peak 2(nm)	Dz(nm)	PDI
Coplymer1	43.5 (100%)	x	43.14	0.117
Coplymer2	29.98 (70 %)	409.2 (28.2 %)	37.18	0.467
Coplymer3	44.3 (76.5 %)	562.4 (23.5 %)	51.52	0.355

From the DLS data, it can be seen that in copolymer1 sample, only one peak at 43.5 nm was detected which was corresponding to the core-shell block copolymer particle. In coplymer2 and coplymer3, there were two families of particles. The small size particles less than 45 nm were created following normal ab initio mechanism as discussed above. On the other hand, the large particles at around 400 nm suggest that there was a secondary nucleation process.

Gel Permeation Chromatography (GPC) Characterization

Gel Permeation Chromatography (GPC) was used to determine the molecular weight and polydispersity of the samples. Prior to analyzing, all the samples were methylated. The carboxylic groups in the polymers were modified by using trimethylsilyldiazomethane as the methylating reagent. This process helps preventing the adsorption of the acrylic acid function to the GPC column of polystyrene [44] as well as facilitate the dissolution of polymer in the eluant. A widely used methylating reagent is diazomethane. However, this involves a very drastic and hazardous procedure which may cause explosion and is very toxic. For this reason we used trimethylsilyldiazomethane as an alternative reagent which required a simpler procedure even though the comparable hazard of the agent still demands extreme care when handling. Furthermore, using trimethylsilyldiazomethane also helped to avoid destroying the trithioester in RAFT polymer structure as it is usually being encountered when using conventional diazomethane especially in the presence of strong bases.

The molecular weight of the samples can be calculated from the retention time upon calibration using polystyrene standard using equation (3)

$$\log M = 9.845 - 0.4339X \qquad \text{equation (3)}$$

In which M is the Molecular weight of polymers, X is the retention time in minutes.

Table 4 and Figure 11 present the results obtained from GPC. Copolymer 1 and copolymer 3 were not analyzed due to the difficulty in dissolving the samples in THF. Alongside are the results obtained by Carvalho [41] who carried out the copolymerization of PAA-TTC with different monomer conversion and butyl acrylate both in solution and in emulsion.

Table 4: GPC results of macroRAFT agents and P (AA-co-BuA) copolymers

a) Our study

System	Mn macroRAFT (Theoretical) g/mol	Mn macroRAFT (Experimental) g/mol	Mn Copolymer (Theoretical) g/mol	Mn Copolymer (emulsion) (Experimental) g/mol
PAA_6TTC	796	1133	19612	41352
$PAA_{60}TTC$	4684	11171	23500	-

b) Carvalho's study.

System	Mn macroRAFT (theoretical) g/mol	Mn macroRAFT (experimental) g/mol	Mn Copolymer (theoretical) g/mol	Mn Copolymer (Solution) (experimental) g/mol	Mn Copolymer (Emulsion) (experimental) g/mol
PAAcoBuATTC 100%	4730	7530	19803	10856	-
PAAcoBuATTC 80%	3857	7718	18930	15920	-
PAAcoBuATTC 70%	3420	7727	18493	23407	-
PAAcoBuATTC 50%	2547	5827	17620	11690	78334
PAAcoBuATTC 20%	1237	5981	15693	-	42674

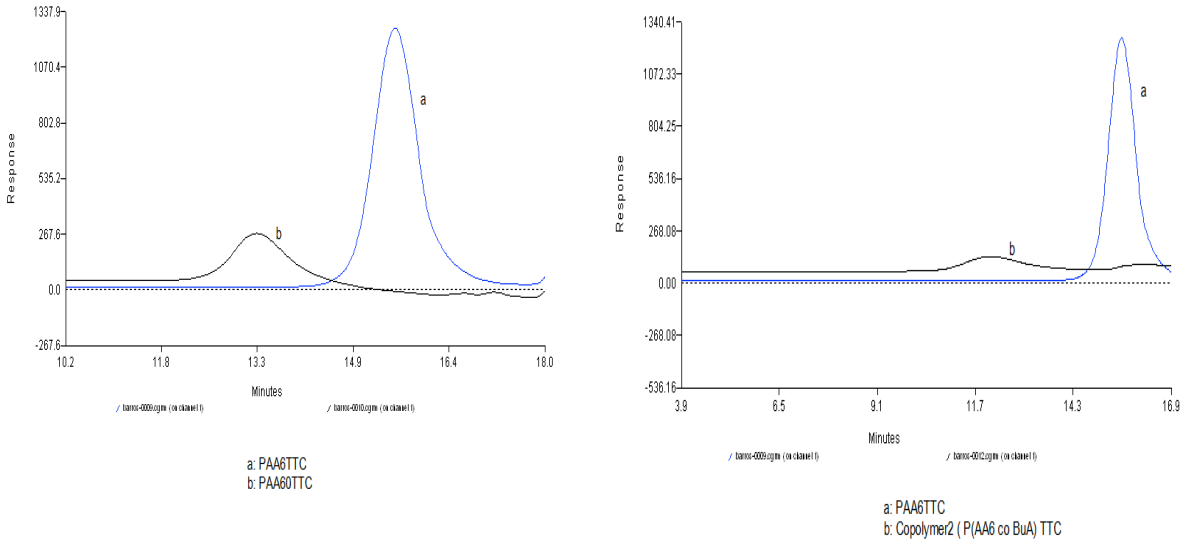

A B

Figure 11: GPC chromatograms of PAA_6TTC vs. $PAA_{60}TTC$ (A) and PAA_6TTC vs.PAA6coBuA (copolymer2) (B)

Figure 11 (A) reveals that with increasing number of the acrylic acid units in the macroRAFT agent from 6 units in PAA_6TTC to 60 units in $PAA_{60}TTC$, the retention time of $PAA_{60}TTC$ was shifted to the lower retention values, meaning an increasing in molecular weight of macroRAFT agent. A similar result is observed in Figure 11 (B). When comparing the retention time of PAA_6TTC with its corresponding copolymer with Butyl acrylate. The shift to the lower retention time of copolymer2 proved the successful addition of butyl acrylate into the macroRAFT agent, indicating the living nature of the system. Mn of $PAA_{60}BuA$ was not measured due to the difficulty in dissolving the copolymer in THF. This difficulty of dissolving $PAA_{60}BuA$ was also observed while attempting to prepare the sample for ^{1}H-NMR using $CDCl_3$. In fact, this insolubility is thought to be associated with crosslinkings. In fact preliminary studies carried out by Barros have already pointed to that probably when AIBN was used as initiator and in higher quantities. Therefore, it is possible that in this case the amount of ACPA used was inadvertly excessive.

From Table 4, it is also noticeable a large variation between the experimental Mn and theoretical one. This large variation can be observed in the case of Carvalho's study while attempting to carry out the copolymerization in emulsion using smaller macroRAFT agent with smaller PAA chain and butyl acrylate suggesting that the polymerization is not really controlled.

In the work of Carvalho, it can be seen that copolymerization in solution gave better results than in emulsion. It was reported that the latex either destabilized or showed multiples peaks on the chromatogram.

Dynamic Mechanical Analysis (DMA) study

The copolymers prepared were studied by DMA. Copolymer 2 was not studied due to the bad quality of the film obtained. The Tgs of $PAA_{60}TTC$, of Copolymer 1 and of copolymer 3 are shown in Figure 12.

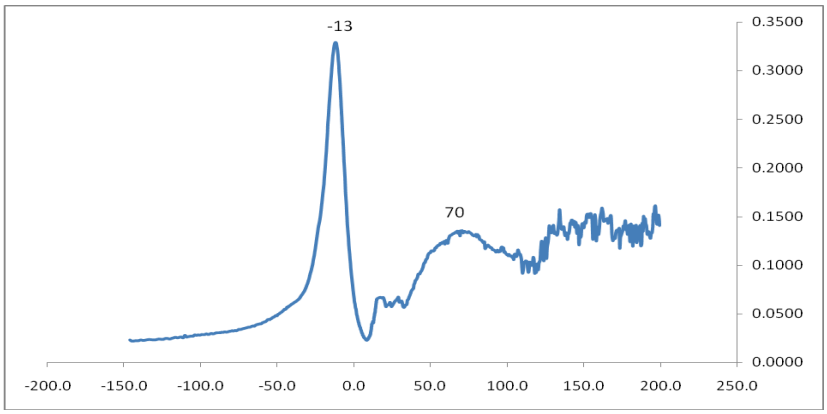

a

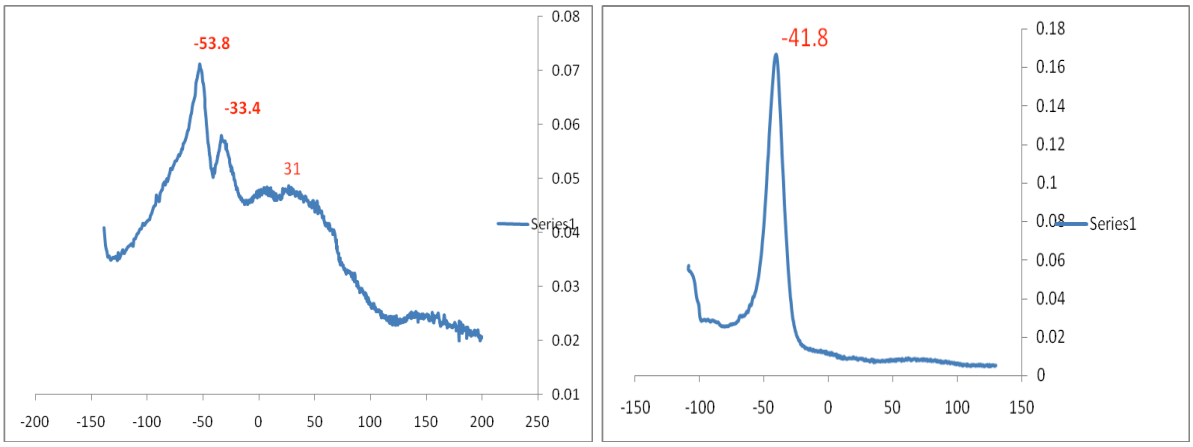

b c

Figure 12: DMA results of $PAA_{60}TTC$ (a), Copolymer1 (b) and Copolymer3 (c)

The macroRAFT agent shows Tgs, one at -13 ^{o}C which might be associated to the C_{12} chain of the RAFT moiety and the other at 70 ^{o}C associated with the PAA chain. For the copolymer samples, two Tg values were expected to be detected corresponding to the

two blocks of the copolymer. According to literature, the butyl acrylate part has a Tg at around – 49 ^{o}C [45] while the Tg of poly (acrylic acid) is at around +105^{o}C [46]. From Figure 12, copolymer 1 showed three Tg values at -53.8 ^{o}C, -33.4 ^{o}C and 31 ^{o}C. The distinctive Tg values indicate the phase separation between the different polymer blocks in the copolymer. The shift of the Tg of the acrylic acid block to lower temperature can be explained by the presence of water in the sample which can act as a plasticizer lowering the Tg of the poly (acrylic acid) block even though a series of precautions were taken such as drying until constant weight in a ventilated oven and samples were kept in a desiccator until use. The presence of a Tg at -33.4 ^{o}C may be due to the cross linking of butyl acrylate chain which might be attributed to the difficulty in dissolving the samples in the solvent while preparing sample for ^{1}H-NMR and GPC. Alternatively, it might result from partial blending of the PBuA block with the PAA block. In the case of copolymer 3, only one Tg appeared at -41.8^{o}C which was higher than the Tg of pure butyl acrylate. In P(AA_6coBuA)TTC the acrylic acid chain was too short to exhibit the characteristic Tg and might blend with the long chain of butyl acrylate, resulting in a single value and shifting the Tg of butyl acrylate to higher value.

Testing the pH – Response of the copolymers

One interesting property which has caught scientists attention is the stimuli-sensitive characteristic of materials, or so called-“smart material”. This type of materials has the ability to response to the changes of external stimuli such as pH of the environment of temperature, resulting in changes in the structure of the material. In fact, it has been reported that poly(acrylic acid) can be used to produce a pH-responsive nanoshells for mesoporous nanocontainer [47]. In our case, the copolymer of acrylic acid and butyl acrylate with the core-shell structure was expected to be pH-responsive. Zetasizer was utilized to determine the dependence of the polymer particles size and Zeta potential as the function of pH. The results are presented in Figure 13

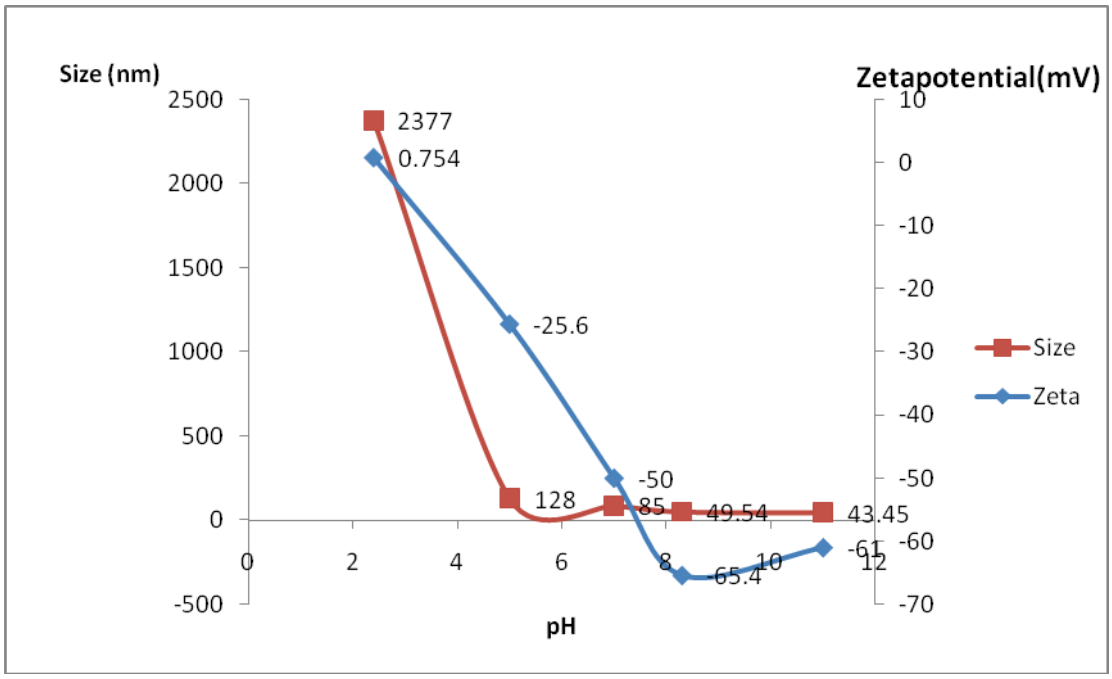

Figure 13: Size and zeta potential of copolymer 1 (PAA_{60}coBuA) as the function of pH

The pH was adjusted at five different values ranging from 2.4 to 11 and at each value of pH, the diameter and Zeta potential of the samples were measured using the Zetasizer equipment at 25°C. From Figure 13 , it can be seen that when the pH was adjusted from low values to higher values, there was a noticeably decreasing trend of the particle size and of the zeta potential. This behaviour can be explained according to the core-shell structure with a hydrophilic poly (acrylic acid) outer shell. At high medium pH, fundamentally, the carboxylate groups are deprotonated and the shell possesses a negative charge responsible for the electrostactically repulsive forces between particles. As a result, the chain extended and the charge density was high. Reversibly, at low pH, the acrylic shell followed a protonation process. Therefore, the charge density was low, resulting in a reduction of the electrostatic repulsive forces between polymer particles. The data trend obtained from Figure 13 was in agreement with the assumed phenomenom. At high pH, the charge density is higher than that at low pH, indicating the denser negative charge presense. Also, the size of the particles also reduceed while increasing pH, verifying the stimuli depending behavior of polymeric particles on the pH. Zeta potential measured at pH=11 was slightly higer than at pH=8. This irregularity may be due to the lack of time needed to stabilze the system.

Copolymer 3 also was tested as a function of pH response. Figure 14 shows the zeta potential of the emulsion with varying pH. A similar decreasing trend of Zeta potential

with increasing pH can be observed, indicating the pH-responsive behavior of the copolymer particles despite of small size the PAA chain.

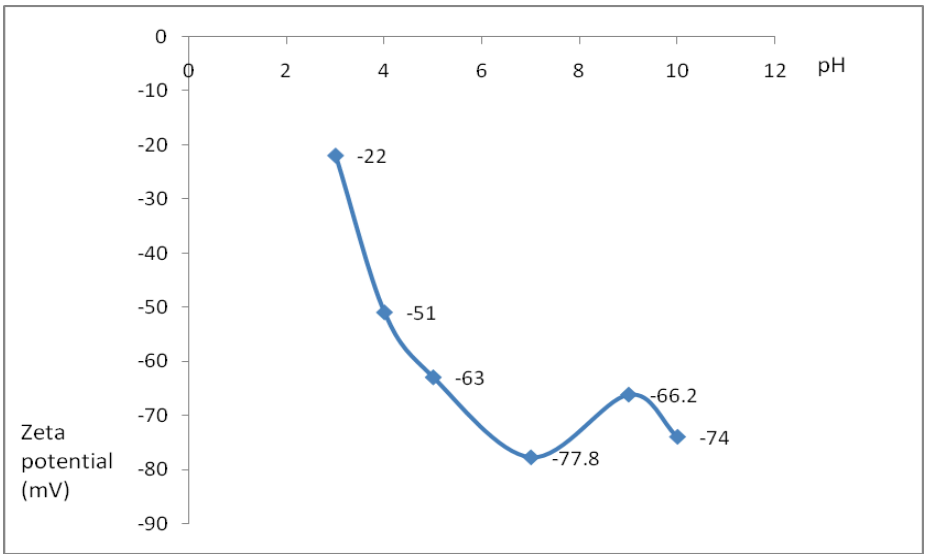

Figure 14: Zeta potential of copoymer3 emulsion as the function of pH

ZnO nanowires

ZnO nanowires were synthesized involving the thermal decomposition of zinc acetate dihydrate following the method of Lin [30]. At high temperature, the crystalline precursors lose the water, converting to volatile compounds and ZnO nanowires were formed and deposited on the wall and the lid of the alumina crucible.

The XRD pattern of ZnO nanowires as shown in Figure 15 had sharp peaks. This indicated that the products contain pure crystalline ZnO without impurities thanks to the fact that catalyst was not used. The crystal structure of the ZnO was determined and lattice parameters were calculated giving a hexagonal close packed structure with lattice constants a=b=3.249 angstroms, c= 5.206 angstroms. From the database, these parameters are in agreement with the theoretical wurtzite structure of ZnO.

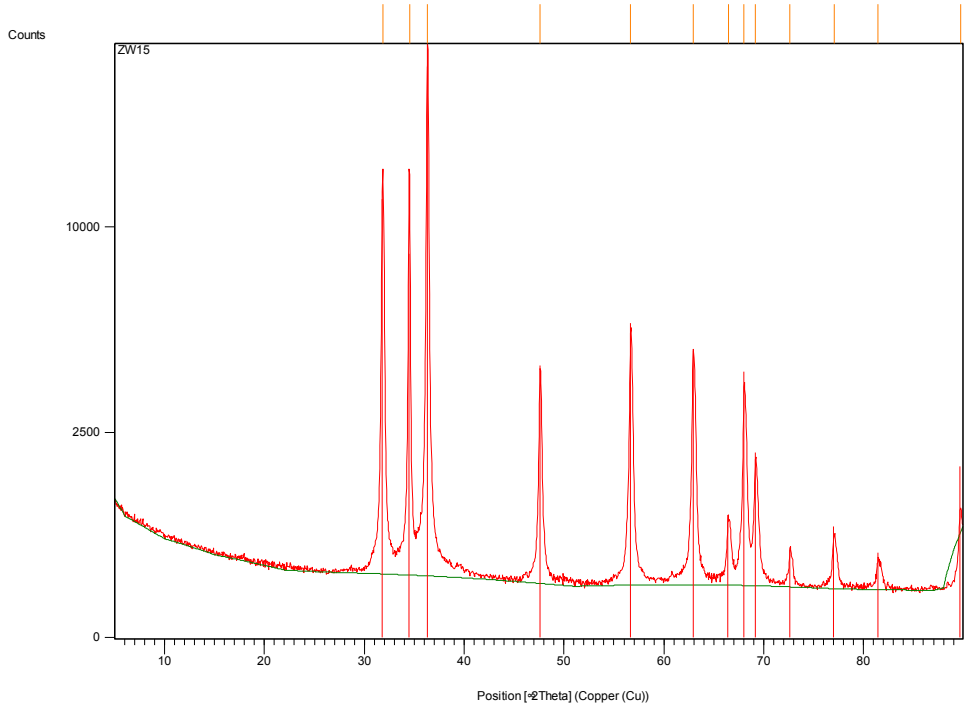

Figure 15: XRD pattern of ZnO nanowires

The SEM images of the ZnO nanowires are shown in Figure 16

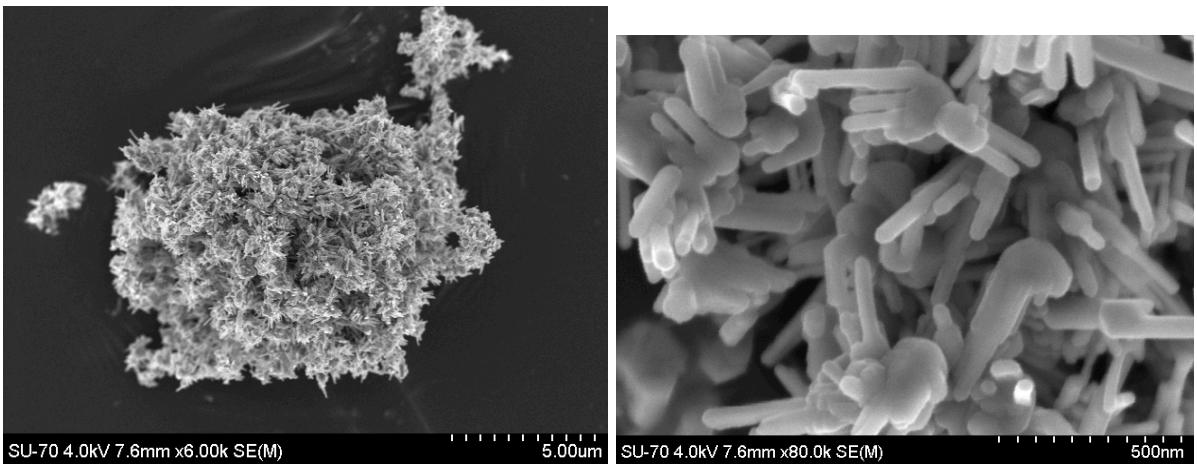

A B

Figure 16: SEM images of ZnO nanowires with different magnifications

As shown in the SEM images the nanowires aggregated into very large clusters. The wires did not show a good aspect ratio as expected. This might due to the fact that the cooling rate could not be controlled because of the technical error of the furnace.

3.1.3. Preparation and characterization of nanocomposites using acrylic acid macroRAFT agents

General review of nanocomposite

Polymer nanocomposites have been widely investigated due to their promising applications. Nanocomposites can be synthesized through various routes such as blending inorganic nanoparticles with polymer or in-situ methods which make use of inorganic precursors and/or monomers.

In our study, the in-situ method was utilized to prepare nanocomposites consisting of nano sized inorganic particles (silica and ZnO) and polymer. The overall procedure is illustrated in Scheme 12.

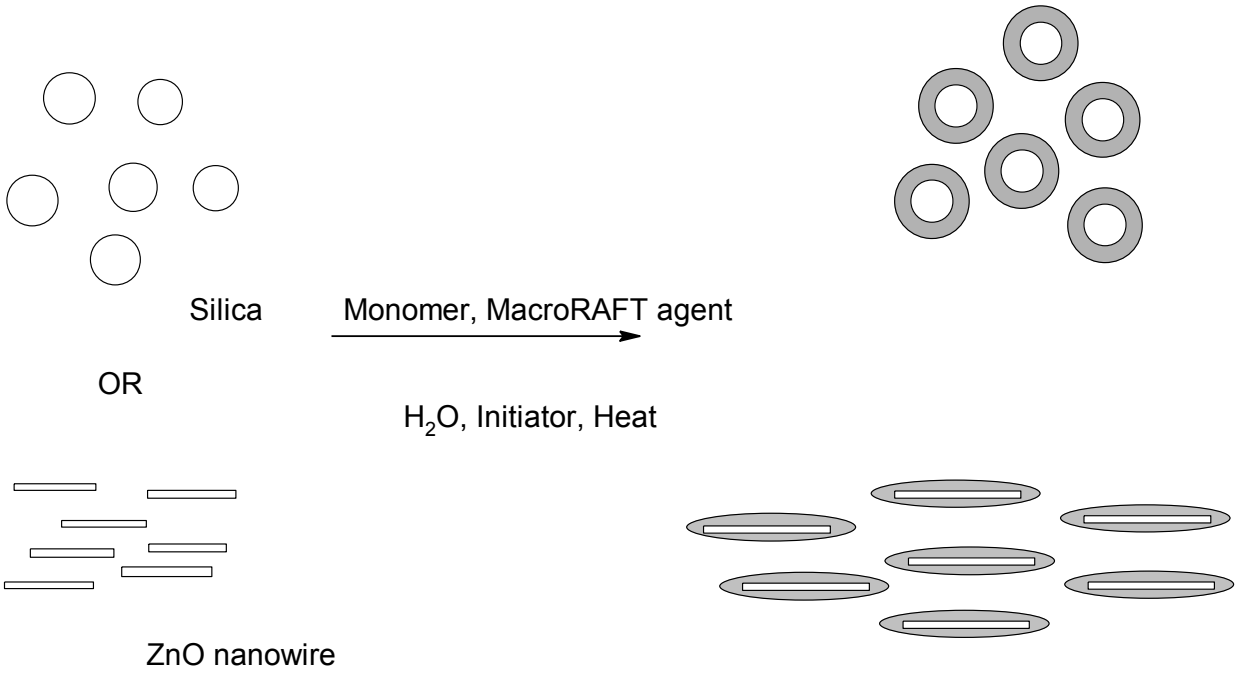

Scheme 12: Overview of nanocomposite formation used in the present study

In our study, nanocomposites were prepared by in situ polymerization method. Silica nanoparticles were previously treated with suitable coupling agents which were 3-aminopropyl trimethoxylsilane (APS) and methacryloxypropyltrimethoxysilan (MPS) in

order to promote interactions between the repeating units of the macroRAFT agent and the silica surface in the first case , and between the growing chain (R*) and the acrylate groups on the silica surface in the case of MPS. ZnO nanowire was used without any modification of the surface. The surface modified Silica nanoparticles or ZnO nanowires were mixed with monomer precursors in aqueous medium. A thermally reactive initiator was then added to commence the emulsion polymerization. In short, the reaction conditions (time of reaction, concentration of organic reagents, temperature) were similar to those used in the preparation of the blank copolymer. The macroRAFT agent was dissolved completely in water after the pH was adjusted to 8. Inorganic fillers with solid content of 5 wt% relative to the monomer mass were added and the mixture was sonicated using either an ultrasound sonication bath or a sonication probe. Table 5 shows the reaction conditions used in the preparation of the nanocomposites:

Table 5: Composites with PAA macroRAFT agents preparation conditions

Composite	**Nanofillers**	**Corresponding blank Copolymers**	**[M]/[RAFT]**	**[RAFT] Mol/Litter**	**[RAFT]/[I]**	**Time (hours)**	**Temperature (^{o}C)**
Sicom1	Silica nanoparticles@APS	Copolymer 1 ($P(AA_{60}$-co-BuA)-TTC	147	0.0084	4	4	70
ZWcom1	ZnO nanowires		147	0.0084	4	4	70
Sicom2	Silica@APS	Copolymer2 ($P(AA_{6}$-co-BuA)-TTC	147	0.0084	4	4	70
ZWcom2	ZnO nanowires		147	0.0084	4	4	70
Sicom3	Silica@APS	Copolymer2 ($P(AA_{6}$-co-BuA)-TTC	147	0.0168	4	4	70
ZWcom3	ZnO nanowires		147	0.0168	4	4	70

Ideally, the mechanism of the preparation can be described as following: first, at high pH, the macroRAFT agent which containes of carboxylate groups was adsorbed on the surface of APS modified silica which possessed positively charged from ammonium

groups leaving the hydrophobic part the macroRAFT on the surface. As the medium is aqueous, a second layer of macroRAFT agent is adsorbed on top to ensure a hydrophilic shell around the particles. Upon addition of butyl acrylate, the monomer diffuses to the interior of this bilayer where the RAFT controlling moiety acts as a chain transfer agent. Then, the RAFT moiety was used to promote the polymerization of butyl acrylate to encapsulate the surface of inorganic particles. Scheme 13 shows the graphical representation of the organic-inorganic nanocomposite preparation process.

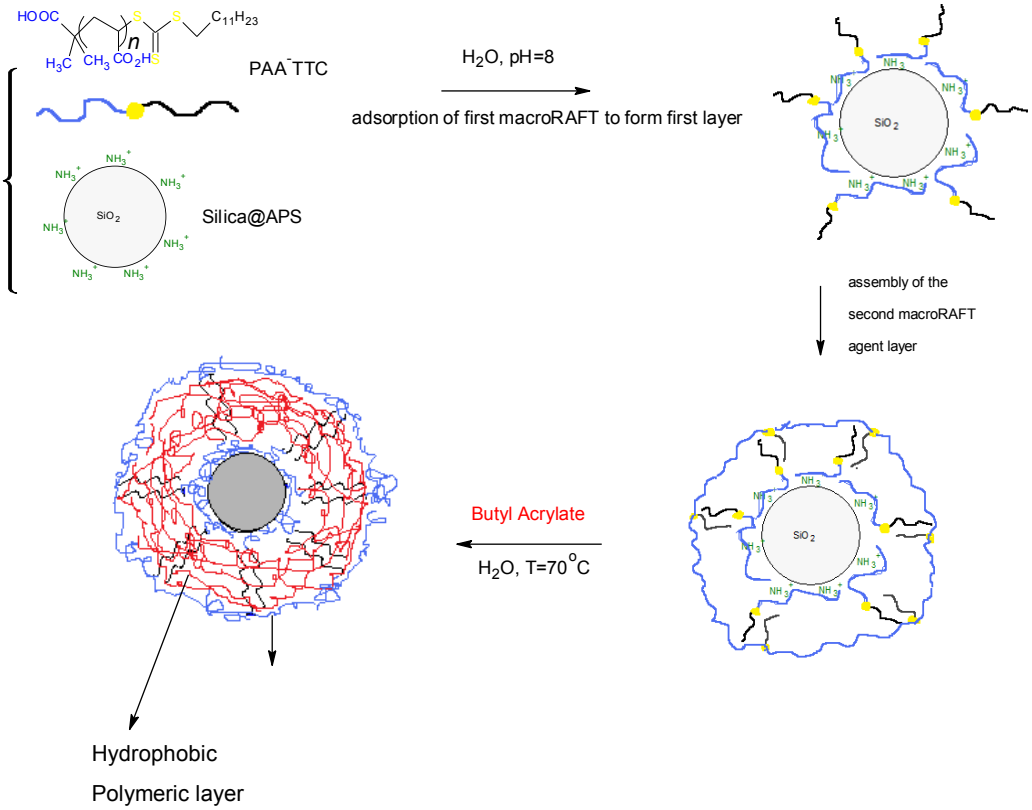

Scheme 13: Mechanism of formation of adlayer-structure hybrid silica nanocomposite

Characterization of Nanocomposite

After the reaction, 1 mL of the latex was withdrawn and spread on a aluminum dish to make a film. Samples from emulsion were characterized by DLS and SEM. The films after being dried were characterized by DMA and FTIR.

Table 6 presents snapshot images of the emulsions and of the films of silica/copolymer and ZnO nanowire/copolymer nanocomposites. Some spaces of DLS data were left blank due to the fact that the polydispersity was so poor that error was reported by the Zetasizer software.

The composite films formed by slow evaporation of water show variation in appearance and mechanical behaviour in comparison with those of the copolymers depending on the type of nanofillers and composition of the copolymers. When prepared with P(AA_{60}-co-BuA)TTC ,the composite of ZnO nanowires showed whiter colour than the silica composite and both were whiter than the blank copolymer. This may due the optical properties of the nanofillers namely those of ZnO. Furthermore, the film with ZnO nanowires was more brittle and less gluey than that of the silica composite which showed no noticeable difference when compare with the film of the blank copolymer. When prepared with P(AA_6-co-BuA)TTC in the same concentration as P(AA_{60}-co-BuA)TTC , the films were more gluey and easily ruptured while peeling than the composite film prepared using P(AA_{60}-co-BuA)TTC. The film with ZnO nanowires was less transparent than the blank copolymer even though it was more yellow than the ZnO nanowires/ P(AA_{60}-co-BuA)TTC. In Sicom3 and ZWcom3, the concentration of both nanofillers and monomers doubled in relation to those used in composite2, the films were more peelable than those composite2, but still more gluey and less brittle than in composite1. From those characteristics, it can be concluded that the long chain of the PAA block helped increasing the brittleness and reduced the glueyness of both composites and blank copolymers, making it easier to peel them than when short chain of PAA was used. Also, the nanofillers reduced remarkably in the transparency of the film.

This peelabe behaviour of the composite films is promising for the preparation of composites using functional nanofillers to be analyzed with proper equipments. In that case, the typical yellow colour of the composite should be removed by destroying the TTC groups by adding proper reagents for example $NaBH_4$ after the polymerization.

As regards the latexes, the DLS study generally showed that two families of particles existed. The big particles were the composite polymer/inorganic fillers while the small particles family may be attributed to the formation of free copolymers particles. These results suggest that an excessive amount of macroRAFT agent was used. Since the DLS method used to measure particles size is limitedly applied to spherical particles, the data obtained for the ZnO nanowires composites are not reliable.

The nanocomposite emulsions did not show good colloidal stability with PDI >>0.01 and precipitated upon a few hours. Generally, samples with ZnO nanowires showed poorer colloidal stability than the samples containing spherical silica.

Table 6: Snapshot images and DLS results of copolymers and nanocomposite using PAA macroRAFT system

CODE	Images	DLS Study		Solid content (mg/mL)	Images
		Z-average	Peaks intensity		
Sicom1		Dz:94.69 PDi: 0.511	Peak 1: 44.94 (51.2 %); Peak 2: 363.0 (48.8 %); pdi: 0.511	137.6	
Sicom2		Dz: 69.64 pdi:0.937	Peak1: 377.8 (58.4 %); Peak 2: 28.2 (37.2 %); peak3: 4824 (4.5%);	161	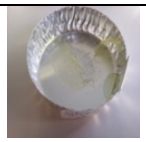
ZWcom1		Dz: 116 PDI:0.544	Peak 1: 321.1 (65.8 %); Peak 2: 47.3 (33.2 %);	136	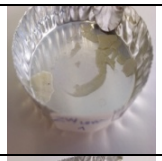
ZwCom2					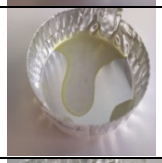
Sicom3		Dz= 555.1 PDI: 0.512	Peak1: 429.7 (91.5%) Peak2: 82 (8.5%)		
ZWcom3		Dz:115 PDI: 0.652	Peak 1: 269 (66.3%) Peak2: 43.54 (43.7%)		

SEM images of nanocomposite samples were taken to assess the distribution of nanofillers in polymer matrix. Figure 17 shows the images of Silica/copolymer nanocomposites.

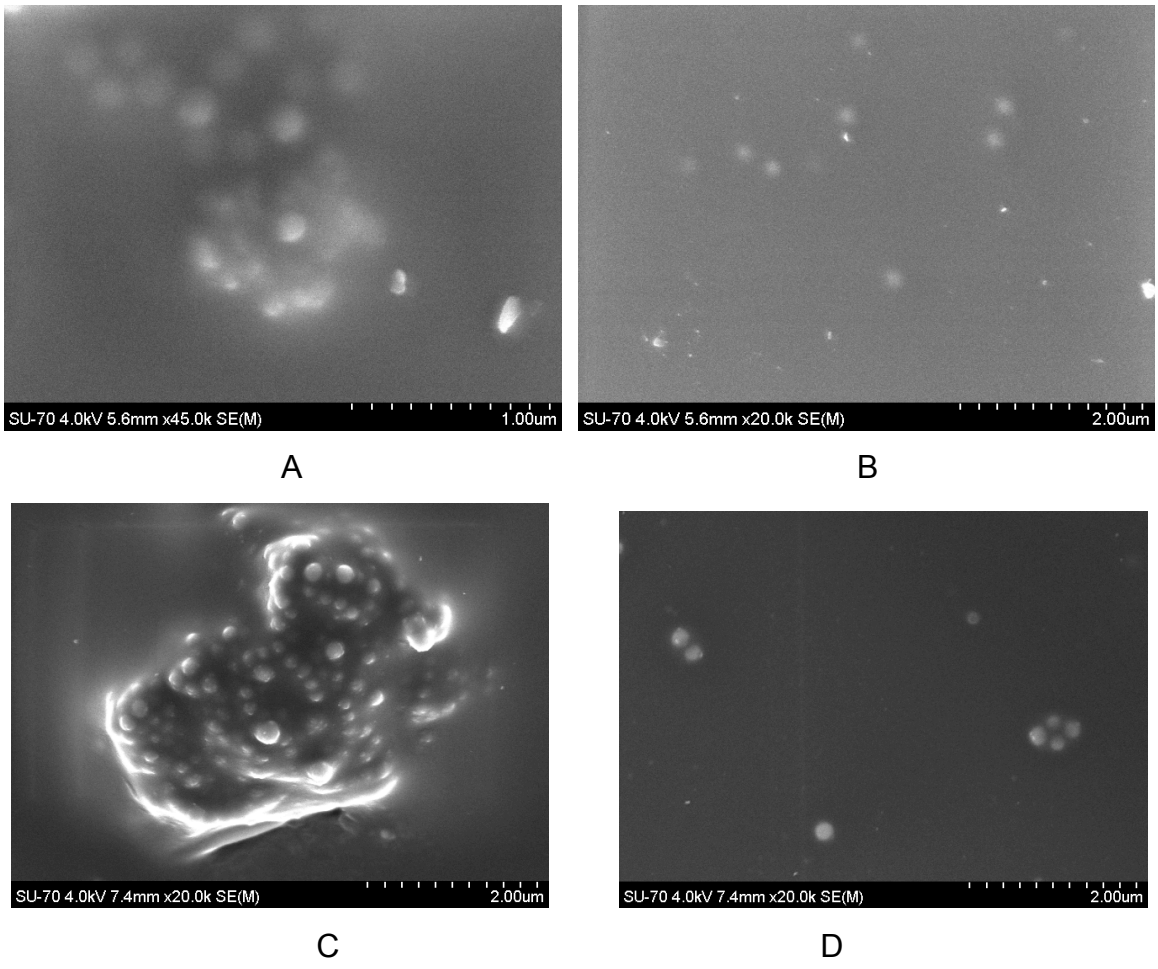

Figure 17: SEM images of nanocomposites: SiO_2 NPs/copolymer1(A)(B); SiO_2 NPs/copolymer 3 (C),(D).

From Figure 17, it can be seen that composite of spherical silica with copolymer P(AA-co-BuA) with size ranging about 300 nm were prepared. Figure 17 (A) and (C) show a cluster of silica spheres covered by polymer while Figure 17(B) and (D) show individual spherical particles. It can be seen that in between the separate spherical particles there is a polymer layer, which confirms that the polymerization was performed on the surface of silica particles. The presence of the clusters in the SEM images may also be the resulted from the improper preparation of the sample. The emulsion might be too concentrated leading to the precipitation of the nanofillers. To achieve more reproducible SEM images, more dilute samples need to be prepared. Figure 18 shows

the second attempt to take SEM image of Sicom1 using a more dilute emulsion. Here, clusters of composite were still observed however with smaller size. An hypothesis for the formation of silica aggregates may involve the bridging of the PAA-TTC molecule over the surface of various silica particles as proposed by Schneider et al. [48]. However, the results obtained for the composites prepared using copolymer3 do not help clarifying this, hence further studies would be necessary.

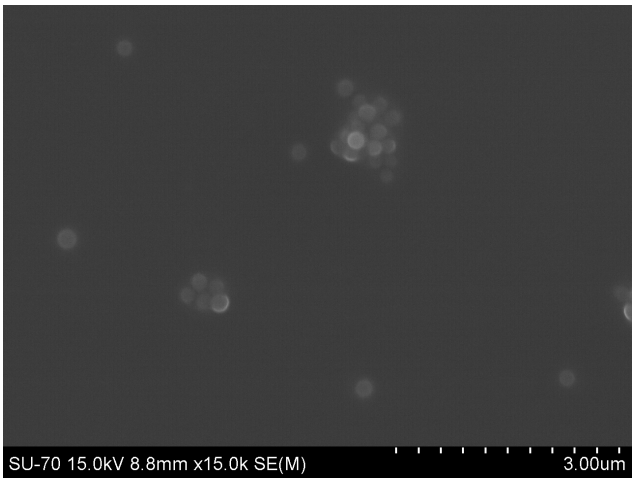

Figure 18: SEM image of Sicom1 (latex more diluted)

SEM images of nanocomposites using ZnO nanowires as fillers are shown in Figure 19

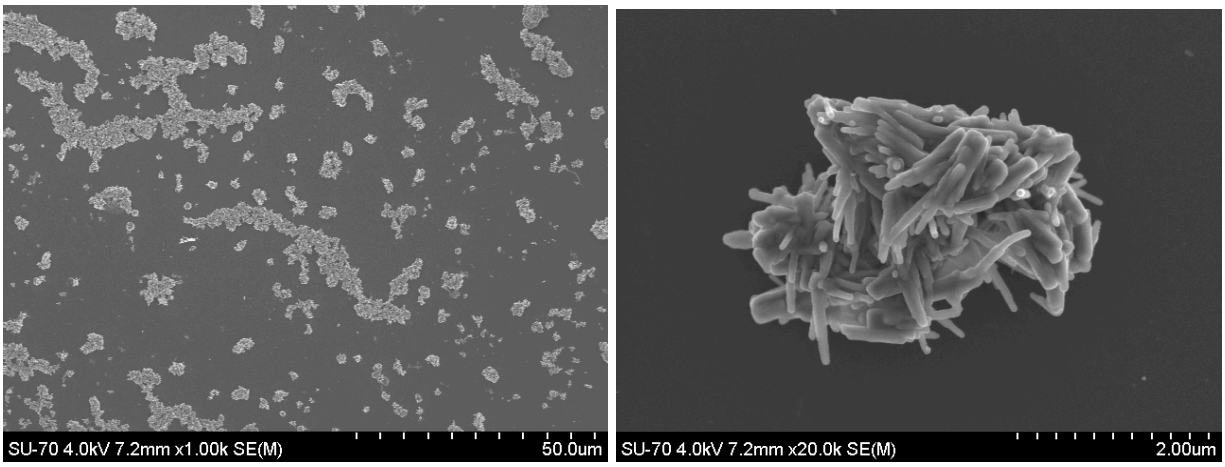

A B

Figure 19: SEM images of nanocomposite of ZnO nanowires as fillers at different magnifications

Figure 19 shows the SEM images of the composites prepared with copolymer 3 (PAA_6-co-BuA) TTC. From Figure 16 ZnO nanowires obtained from the thermal decomposition

of Zinc acetate dehydrate aggregated into clusters. Therefore the nanowires did not separate in the nanocomposite as seen in Figure 19 A and B even sonication using a probe had been performed on the mixture of ZnO nanowires and macroRAFT agent solutions prior to copolymerization reaction occurred. Hence, an optimized process to prepare isolated nanowires needs to be investigated further in order to obtain better composite.

In order to detect precisely the presence of the polymer layer, TEM analyses are required, however due to the limited access to the equipment; TEM was not possible to perform in this study.

DMA was used to investigate the effect of the nanofillers on the Tg of the polymers. The results are presented in Table 7 and compared with the data of the corresponding blank polymers.

Table 7: DMA results of composites and blank copolymers samples

Samples	Tg1	Tg2	Tg3
Copolymer1	-53.8	31	-33.4
Sicom1	-58	50	x
Zwcom1	-65	57	x
Copolymer3	-41.8	x	x
Sicom3	-42	x	x
Zwcom3	-42.7	x	x

From Table 7, in both blank copolymer1 and Sicom1 and ZWcom1, the Tg of PAA block appeared in the high temperature region. As regards the PBA block, in the composite samples the Tgs of butyl acrylate part in were detected at lower values. This suggests that in the presence of Silica nanoparticles, the Tgs of the two blocks were more separated, indicating a higher degree of phase separation. This may own to the interaction between the nanofillers and the hydrophilic hard part of the copolymer.

In the case of copolymer 3 and its corresponding nanocomposites, only one Tg was detected near -42^{o}C whilst the Tg of the PAA block was not detected. This absence of Tg of PAA blocks may due to the fact that the PAA was too short. Also, two polymer blocks may blend with each other, resulting in the shift of Tg to a higher value comparing with pure butyl acrylate.

DMA analyses were not performed on samples of copolymer 2 and its corresponding composites since the films were too gluey and easily ruptured to be analyzed by DMA equipment.

Studying the pH- response of nanocomposites

Similar to copolymer samples, the nanocomposite samples containing the poly (acrylic acid) part on the outer shell as presumed in scheme 13 is expected to exhibit pH-responsive behaviour. DLS and zeta potential measurements were performed only on Silica composite 1. Silica composite 2 and 3 were not studied due to constraint of time. The results are shown in Figure 20.

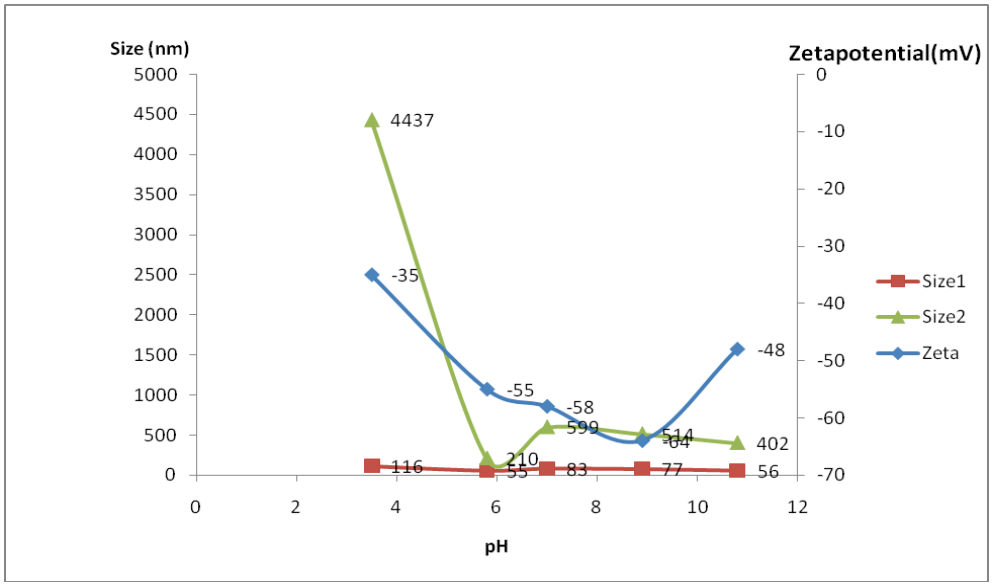

Figure 20: Plot of pH- responsive behavior of silica composite 1

From the results obtained, the zeta potential of silica composite 1 showed negative values in the whole range of pH values. As the results indicate, when increasing the pH of medium, the Zeta potential shifted to more negative values. This behaviour is due to the deprotonation of carboxylic groups in high pH indicating that the acrylic acid chains were present on the surface of the particles, causing the pH-responsive phenomenon. The elevated zetapotential value at pH=11 comparing with pH=8 may be due to the lack of required time to stabilization.

From the results obtained, especially from SEM and DLS, the nanocomposites containign Silica nanoparticles and ZnO nanowires did not exhibit good colloidal stability. In the case of ZnO nanowires, the agregation of the nanofillers before being used to prepare nanocomposite was the main reason of the final agregation in nanocomposite. Therefore, further optimization to prepare isolated ZnO nanowires needs to be studied.

As regards the nanocomposites containing Silica@APS, eventhough the surface of the silica was treated with suitable groups to promote better interaction with the copolymers, the loss of colloidal stability was still observed. Presumed explainations can be given as following:

- Acrylic acid-based macroRAFT agents which possess a large amount of deprotonable carboxylic groups, may be subjected to the unexpected eclectrostactic sheer while changing the medium environment.
- PAA_{60}TTC due to its large morlecular weight might bridge over several silica nanoparticles instead of wrapping individual particle due to the excessive length of the hydrophilic acrylic acid chain which acted as a long a polyelectrolyte , leading to the coagulation of the inorganic parts in the final emulsion. This bridging flocculation effect was also disscussed by Schneider et al. [48]
- Attempts to use a a macroRAFT agent with reduced chain length was done with PAA_6TTC. However, in this case the hydrophilic part seems to be too short to act as a stabilizer, resulting in aggregation/precipitation.

To overcome the above problems with acrylic acid – based macroRAFT agents, and being inspired by the work of Boisse et al. [22], two new macroRAFT agents were prepared . One agent was composed of poly(ethylene glycol) segments and the other was composed of a random distribution of acrylic acid and poly(ethylene glycol) segments. The repeating units of the new macroRAFT agent were tuned at around 40 units, assuring an appropriate chain length. The random distribution of poly(ethylene glycol) segment and acrylic acid segment was to avoid the adverse dependence of the polyeclectrolyte to the changing environment and also to prevent phase separation.

3.2. Poly (ethylene glycol)-based macroRAFT agent system

Poly (ethylene oxide) has been used successfully as a hydrophilic part making up the macroRAFT agent. In this context, the group of Charleux [17, 21, 22] has performed the esterification of the trithiocarbonate RAFT agent TTC-A with poly (ethylene oxide) to form PEO-TTC. This macroRAFT agent was used to control the copolymerization with n-butyl acrylate in emulsion. The authors were capable of tuning the size of the copolymer and the molecular mass by simple changing the molar ratio between the PEO-TTC macroRAFT and the hydrophobic monomer. In another work, Boisse et al. [22] produced novel structural macroRAFT agent which consisted in a random

distribution of acrylic acid (AA) and poly(ethylene glycol) methyl ether acrylate (PEGA) units. This macroRAFT agent was used as the chain transfer agent for polymerization of poly (styrene).

3.2.1. Preparation and characterization of PEGA-based macroRAFT agents

Inspired by such previous works, in our study, we attempted to prepare two macroRAFT agents: one with only PEGA and the other was composed of an equivalent number of repeating units of both AA and PEGA distributed randomly. Table 8 shows the reaction conditions used for preparing the two macroRAFT agents.

Table 8: PEGA- based macroRAFT agents preparation conditions

Code	Monomer	[AA]/[RAFT]	[PEGA]/[RAFT]	[RAFT]/[I]	[RAFT] (Mol/L solvent)	Time (hours)	Solvent	Temperature (^{o}C)
MacroRAFT3	Poly(ethylene glycol) methyl ether acrylate (PEGA)	x	44	14	0.000109	4	Ethanol	70
MacroRAFT4	AA + PEGA	22	22	14	0.000109	1	Ethanol	70

Comparing with the reactions to prepare macroRAFT agents using PAA as shown in table 1, the preparation of PEGA-TTC had some differences which are: instead of DMF, ethanol was used as solvent which is easier to remove after the reaction; the time need to prepare PEGA-TTC was higher than PAA-TTC and P(AA-PEGA) TTC because the reactivity of PEGA monomer was lower. The ratio of the concentration of RAFT and initiator in preparing PEGA-TTC was higher than in preparing PAA-TTC.

After the reaction, the products were precipitated from cold diethyl ether to remove any trace of unreacted monomer as well as solvent. The dried polymeric products were characterized by ^{1}H-NMR, FTIR, DMA and GPC.

The FT-IR spectrum of PEGA-TTC shows that there was a decreasing in the intensity of the peak at 1636 cm^{-1} assigned to the C=C in monomer, indicating that homopolymerization occurred yielding the macroRAFT agent. See Annex 3 and 4.

Figure 21 and Figure 22 show the ^{1}H-NMR spectra of the two macroRAFT agents.

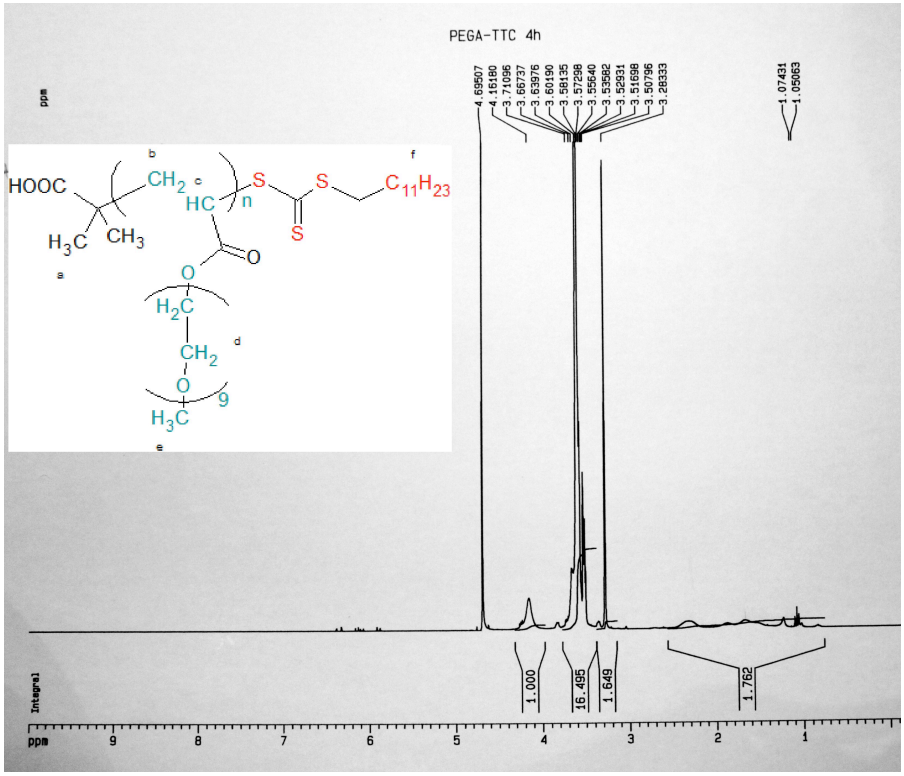

Figure 21: ^{1}H-NMR spectrum of P(PEGA) – TTC

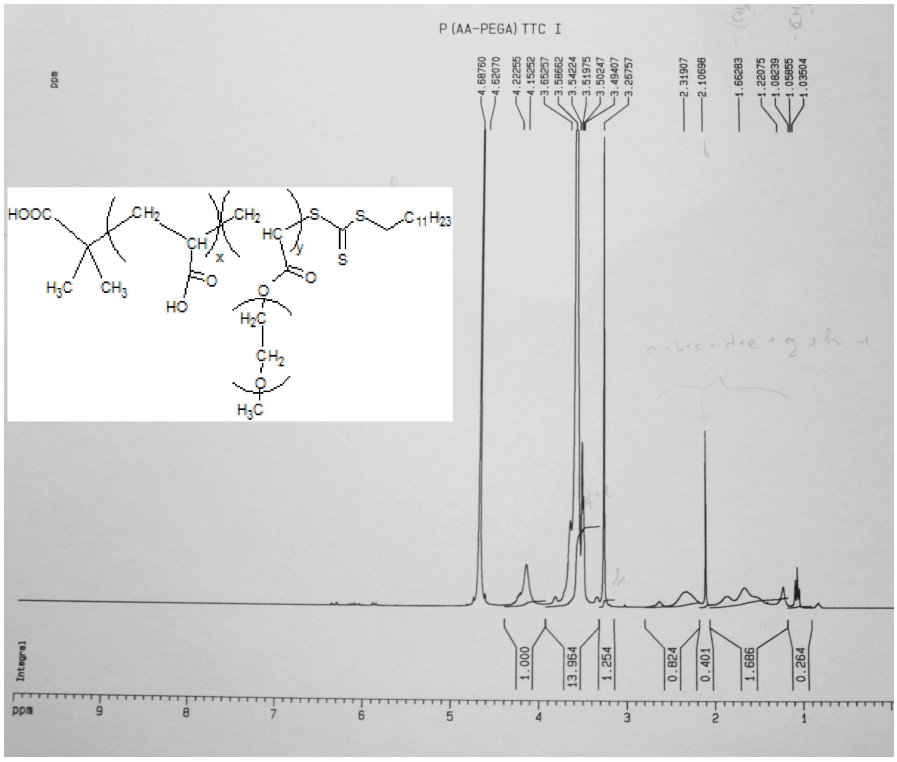

Figure 22: ^{1}H-NMR spectrum of P(AA-PEGA) – TTC

The corresponding chemical shifts of both polymeric part and TTC part were present in both spectra, proving the successful link of the polymeric part to the trithiocarbonate group. In the ^{1}H-NMR spectrum of P(PEGA)TTC, the TTC part was confirmed by the peaks in the range of 0.8 to 2.3 ppm. In spectrum of P(AA-PEGA) TTC, the increase of integral of the peak at 2.4 ppm denoting to the presence of acrylic acid repeating units.

The ^{1}H-NMR spectra were also used to calculate the degree of polymerization and the molecular weight of the macroRAFT agent. The molecular weight was calculated based on the ratio of the integral of the proton signals of the poly(ethylene glycol) at 3.5 ppm and the integral of the protons signal of TTC. It was calculated from Figure 21 that the degree of polymerization of PEGA was 36 which corresponding to the molecular weight of P(PEGA)-TTC of 17344 g.mol^{-1}; from Figure 22 the degree of polymerization of PEGA was 22 and AA was 20 which corresponding to the molecular weight of 12364 g/mol.

GPC was performed to determine the molecular weight of the macroRAFT agent upon methylation of all the samples. The results are shown in Table 9.

Table 9: **GPC results of the PEGA-based macroRAFT agent, the theoretical molecular weight and the molecular weight calculated by proton-NMR**

MacroRAFT	Mw(Exp) (g/mol)	Mn(Exp) (g/mol)	PDI	Mn(Theo) (g/mol)	Mn(NMR) (g/mol)
PEGA-TTC	5169	4040	1.27	21418	17644
P(AAPEGA)-TTC	3677	3256	1.12	12508	12364

From the GPC results, the macroRAFT agents showed molecular weight lower than the theoretical ones and calculated from proton NMR. However, the homopolymer PEGA and the copolymer P(AA-PEGA) showed a relatively narrow molecular weight distribution with PDI of 1.27 and 1.12 respectively. This discrepancy between the calculated molecular weight and the experimental ones may be associated with the analytical conditions used, in particular the type of standards which bare little resemblance to the polymers analysed.

DMA analysis was performed to study the Tgs of the two MacroRAFT agents. Figure 23 shows the results.

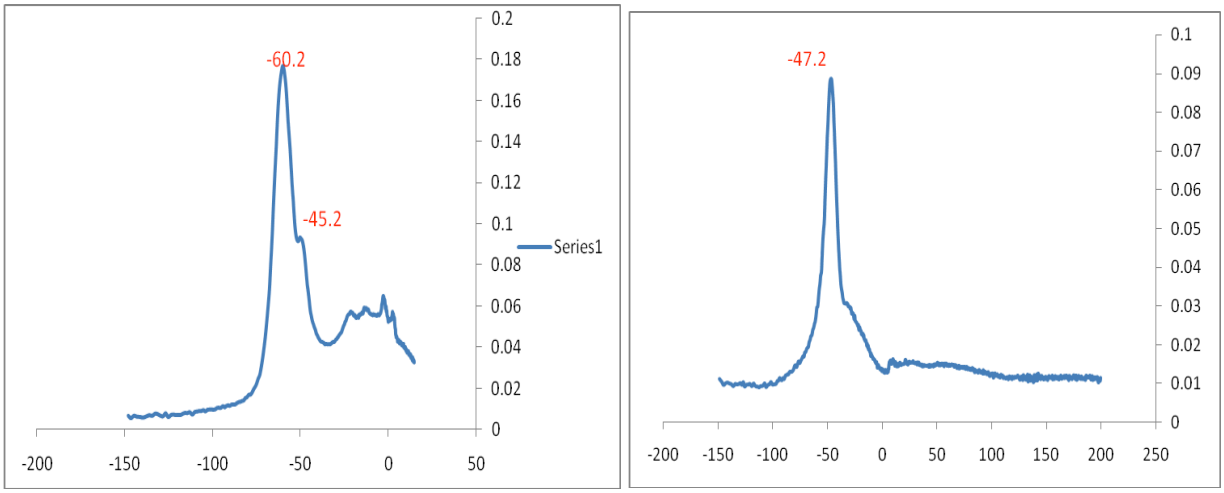

a b

Figure 23: DMA of P(PEGA)-TTC (a) and P(AA-PEGA)-TTC(b)

The Tg of P(PEGA)TTC was detected at -60.2 ^{o}C which is in agreement with the flexible poly (PEGA) block. In the case of macroRAFT4 (PAA-PEGA-TTC), the acrylic acid and PEGA units are thought to be randomly distributed due to the simultaneous addition of monomers when preparing the macroRAFT agent and similar reactivity ratios. In fact, the presence of a single Tg at -47.2 ^{o}C, a much higher value than that of pure PEGA in P(PEGA)-TTC is in agreement with a random distribution of the two repeating units and the effect of the more rigid AA repeating units. Notice should be made about the presence of the shoulder at -45.2 ^{o}C in the case at the P(PEGA)-TTC which may be associated with the local interaction with the C_{12} of the RAFT moiety and/or the difference in the mobility between the main chain and the pendant PEG groups. In the case of P(AA-PEGA)TTC such shoulder is hardly noticed. The noise in the region near 0 ^{o}C may be due to the presence of water in the samples which showed a phase transition at near 0 ^{o}C.

3.2.2. Preparation and characterization of copolymers using PEGA- based macroRAFT agents.

Following the same procedure used to prepare copolymers using acrylic acid-based macroRAFT agents, the PEGA-based macroRAFT agents were used to synthesize copolymers with butyl acrylate and methyl methacrylate. Table 10 shows the reaction parameters used to prepare the copolymers. pH was only adjusted to 8 in the case of using P(PEGA-AA) in order to facilitated the dissolution of macroRAFT agent which contained carboxylate groups.

Table 10: Copolymerization using PEGA macroRAFT agent

Reference	macroRAFT agent	Monomer	[RAFT]/[I]	[RAFT] (mol/L solvent)	[M]/[RAFT]	Time (hours)	Temperature (^{o}C)	pH
Coplymer4	PPEGA-TTC	Butyl Acrylate	4	0.084	147	4	70	7
Coplymer5	PPEGA-TTC	Methyl Methacrylate	4	0.084	147	4	70	7
Coplymer6	P(PEGA-AA)TTC	Butyl Acrylate	4	0.084	147	4	70	8

After the reaction, a film was made from 1 mL of emulsion on a disposable aluminum dish and dried overnight in a ventilated oven at 60 ^{o}C until constant weight. Parameter of the film was characterized by DMA, the remaining was used to prepare solutions for ^{1}H-NMR and GPC. The emulsion was analyzed by SEM and DLS.

Characterization

^{1}H-NMR was performed on the copolymer 4 and copolymer 6 after dissolving the samples in $CDCl_3$. The spectra are presented in Annex 5 and 6. Comparing with the spectra of TTC-A and macroRAFT agents, in the copolymers, both characteristic peaks of TTC and PEGA and AA appeared in the spectra. In both copolymer 4 and copolymer 6, the ratio of the integral of the peak at the region of 2.14 ppm which is corresponding to the of methylene proton Hα, and integral the peak at 3.5 ppm which corresponding to CH_2CH_2-O- of the PEG is higher than that in the spectra of macroRAFT agents as shown in Figure 21 and Figure 22. This increase indicates the presence of butyl acrylate in the samples, confirming the copolymerization.

DLS was used to study the particles size and size distribution of the copolymers in the emulsion. The results are shown in Table 11

Table 11: DLS of copolymers using PEGA-TTC and P(AA-PEGA)TTC as macroRAFT agents

Samples	Z-average (nm)	Peak 1(nm)- Percentage (%)	Peak2 (nm) – Percentage (%)	PDI
Copolymer4	Dz: 99.43	180 (100%)	-	0.393
Copolymer5	Dz: 98.19	101(100%)	-	0.008
Copolymer6	Dz: 114	144 (98%)	27 (2%)	0.194

From Table 11, the DLS results reveal that the main peaks here are much bigger than for PAA-TTC systems as shown in Table 3. This may due to the fact that the comb-like structure of PEGA-based macroRAFT agents is much bigger than the linear PAA macroRAFT agents resulting in bigger copolymer particles.

The pH – responsive behaviour of copolymer6 was studied to investigate the role of acrylic acid repeating units on the morphology of the polymer particles at different pH values. Size and Zeta potential of the emulsion were measured at different pH using the Zetasizer. The results are shown in Figure 24.

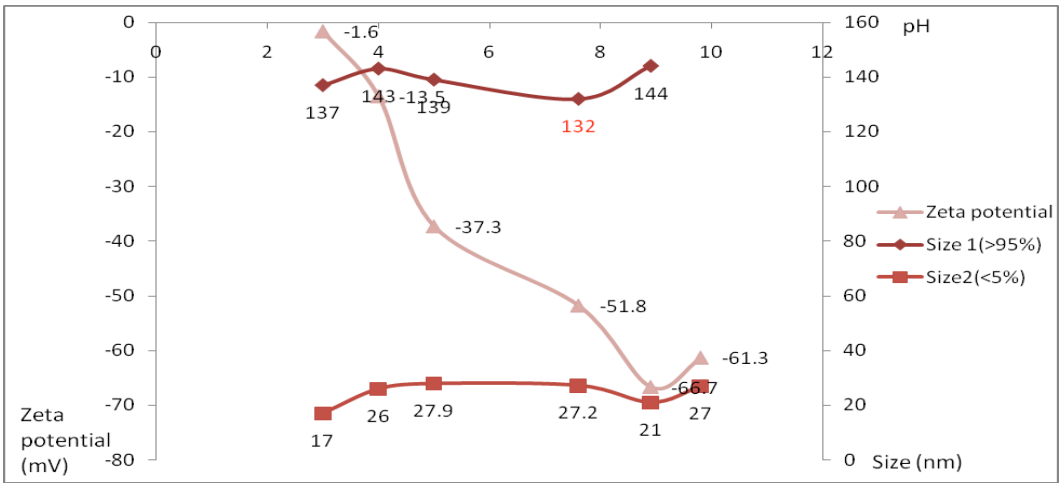

Figure 24: Size and Zeta potential of copolymer 6 emulsion as function of pH.

As shown in Figure 24, when increasing the pH of the emulsion, the Zeta potential values of the particles moved to more negative values, indicating a denser negative charge on the surface of the particles which was driven by the presence of carboxylate

groups on the surface of the particles. This phenomenon is in agreement with the presumed mechanism of the core-shell structure formation discussed for the copolymers with PAA-TTC. The size of the particles was found not to change significantly with varying the pH. This behaviour was different from the copolymer P(AA-co-BuA) in which the dependence of the particles size on the pH was found remarkable. In the case of P(AA-PEGA-BuA) copolymer, the presence of PEGA units in random distribution with AA units helped to prevent the coagulation of the polymeric particles even when the absolute Zeta potential values were low.

GPC was performed on all copolymer samples to determine the molecular weight of the products. Methylation was carried out on all samples prior to the measurement. The results can be found in Table 12 and Figure 25

Table 12: GPC results of macroRAFT agent and corresponding copolymers

MacroRAFT	Mw(Exp) (g/mol)	Mn(Exp) (g/mol)	PDI	Mn(Theo) (g/mol)	Mn (NMR) (g/mol)	Copolymer	Mw(Exp) (g/mol)	Mn(Exp) (g/mol)	PDI	Mn(Theo) (g/mol)
PEGA TTC	5169	4040	1.27	21418	17644	Coplymer4 (P(EGA-BuA)	10457	9886	1.05	40234
						Coplymer5 (PEGA-MMA)	4863	4357	1.11	36128
							24340031	x	x	
P(AAPEGA) TTC	3677	3256	1.12	12508	12364	Coplymer6 (PAA-PEGA-BuA)	50499	x	x	31324

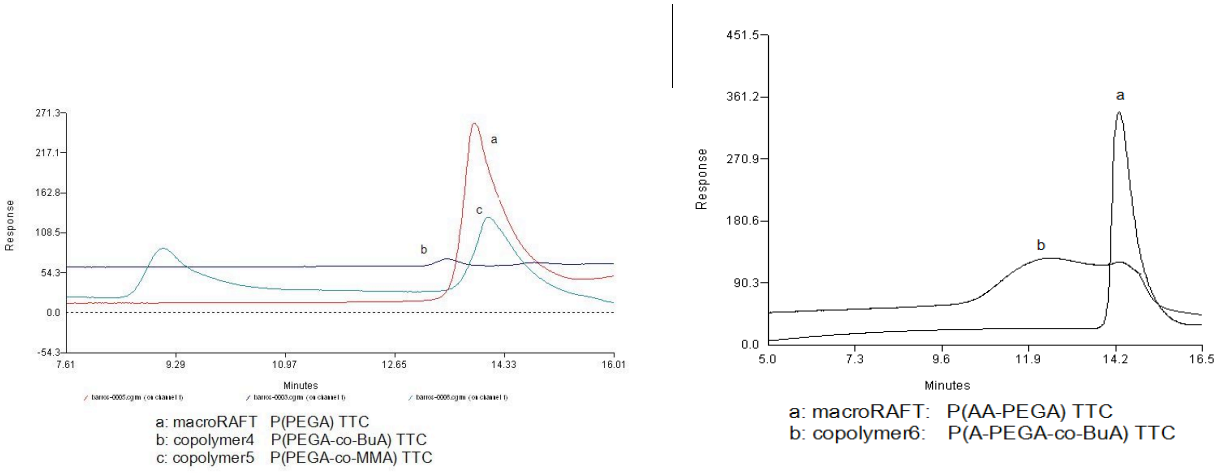

A B

Figure 25: GPC chromatograms of macroRAFT agents and corresponding copolymers.
A: P(PEGA) TTC versus P(PEGA-co-BuA) TTC and P(PEGA-co-MMA) TTC
B: P(AA-co-PEGA) TTC versus P(AA-co-PEGA-co-BuA)TTC

In Figure 25 (A), the shift of retention time of copolymer4 to the left side comparing with the peak of P(PEGA)TTC confirms the copolymerization with butyl acrylate, proving the livingness of the system. The Poly Dispersity Index of copolymer 4 was found unusually lower than that of macroRAFT agent; this may due to the purification procedure which may have allowed removal of smaller polymer chains. Once again, the discrepancy between the calculated values for Mn and those determined is striking and are thought to be due to the analytical conditions used as discussed before. Unfortunately conversion data were not determined to substantiate this hypothesis. Yet notice should be made to the fact that the value calculated based on the 1H-NMR spectrum is in reasonable agreement with the theoretically calculated indicating that conversions were high.

For copolymer5, the two distinctive peaks were obtained. One peak was at the same position of the macroRAFT agent and the other corresponding to very high molecular weight. This indicates that the copolymerization did not occur under RAFT conditions. Instead, free radical homopolymerization of PMMA occurred. The phenomenon is thought to be due to poor blocking efficiency between the acrylate system and the methacrylate system in a copolymerization process. This may be explained by the difference in the rate of initiation between methacrylate and acrylate monomers. In which the rate of propagation of the second block is far faster relative to the rate of initiation [49].

Figure 25 (B) indicates a higher molecular weight of copolymer 6 than its corresponding P(AA-PEGA) TTC macroRAFT agent. However the peak is broad and the presence of a shoulder corresponding to the macroRAFT agent suggests that this reaction was not well controlled.

DMA was carried out on copolymers after the samples were dried until constant weight in a ventilated oven at 60^{o}C to remove any trace of moisture. The results obtained are shown in Figure 26.

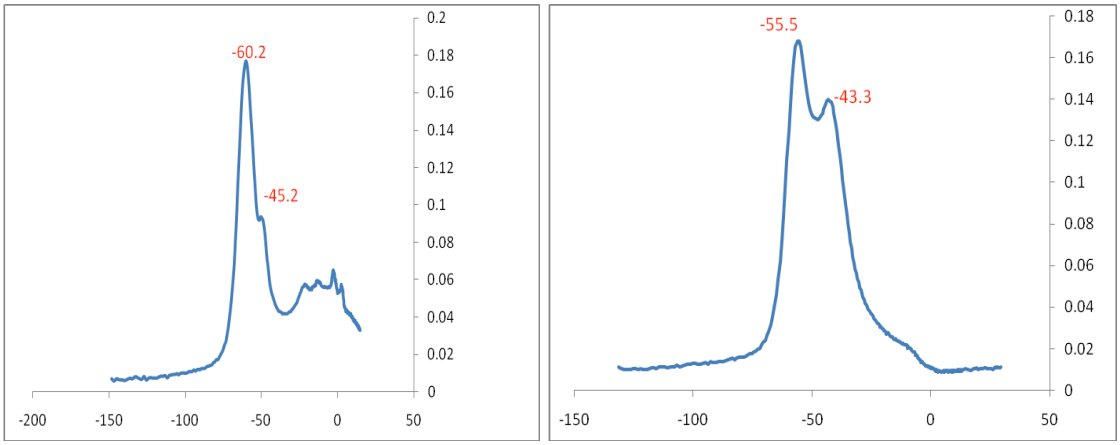

A: PEGA-TTC macroRAFT agent

B: copolymer4 (PEGA-BuA)TTC

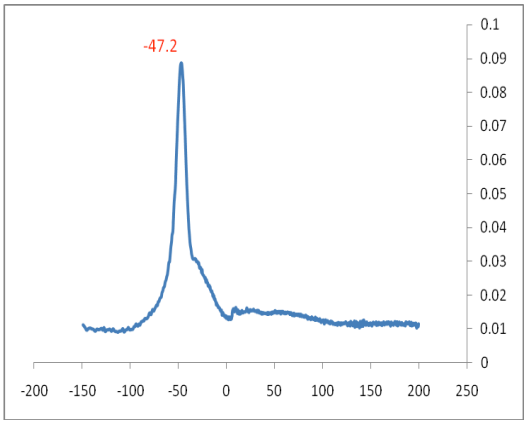

C: P(PEGA-AA)TTC

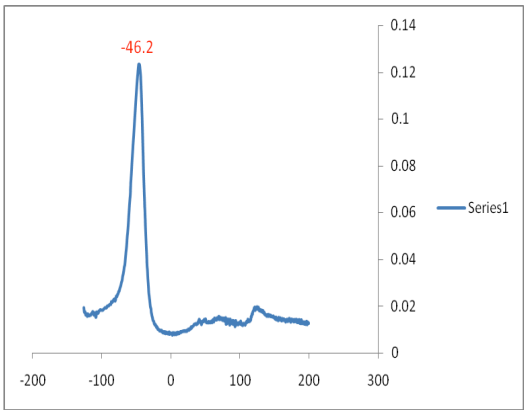

D: copolymer 6 – P(PEGA-AA-BuA)

Figure 26: DMA results of macroRAFT agents and their corresponding copolymers.

From Figure 26, copolymer 4 presented two Tgs associated with the PEGA block (-58^{o}C) and the butyl acrylate block (-43.4^{o}C), proving the formation of the copolymer with two distinctive blocks. In the case of copolymer 6 upon addition of butyl acrylate to the P(AA-PEGA)-TTC macroRAFT agent, only one Tg was detected at -46.2 ^{o}C. As discussed earlier the hydrophilic part composed of random distribution of AA and PEGA exhibited only one Tg value at -47 ^{o}C, higher than that of pure P(PEGA) and closer to the Tg of the pure poly (butyl acrylate). Therefore, the Tg of the newly added butyl acrylate block is thought to be mixed with the random chain of the macroRAFT. This phenomenon was not detected in case of P(PEGA-co-BuA), hence, it can be presumed that the presence of acrylic acid contributed to this blending.

3.2.3. Preparation and Characterization of nanocomposite using silica nanoparticles and PEGA-based macroRAFT agents

Preparation

PEGA-TTC and P(PEGA-AA)-TTC were used as macroRAFT agents to prepare nanocomposite containing Silica nanoparticles and copolymer4 and copolymer6. The silica nanoparticles were coated by two different surface coating agents : APS and MPS in order to promote the interaction between polymer and particles. The composition and reaction conditions are summarized in Table 13

Table 13: Nanocomposites preparation using PEGA macroRAFT agent

Reference	macroRAFT	monomer	Fillers	[RAFT]/[I]	[RAFT] (mol/L solvent)	[M]/[RAFT]	Time (hours)	Temperature (^{o}C)	pH
Sicom4	PEGA-TTC	BuA	SiO_2@APS	4	0.084	147	4	70	7
Sicom5	PEGA-TTC	MMA	SiO_2@APS	4	0.084	147	4	70	7
Sicom6	PEGA-AA-TTC	BuA	SiO_2@APS	4	0.084	147	4	70	8
Sicom7	PEGA-TTC	BuA	SiO_2@MPS	4	0.084	147	4	70	7

The conditions of the reactions were similar to those used in the preparation of blank copolymers. pH was adjusted to 8 in the case of sicom6 to promote the deprotonation of the acrylic acids units, yielding a negative charge of the macroRAFT agent which may be adsorbed onto the positively charged surface of Silica@APS. The composites were characterized by SEM, DMA and DLS.

Characterization

Similar to the composites prepared with PAA macroRAFT agents, the appearance and mechanical properties of the films were examined. Generally, comparing to the blank copolymers and the composites with PAA-systems, the PEGA systems films were less peelable, more gluey and ruptured easily. The composites and the blank copolymer with P(PEGA-co-AA-co-BuA)TTC showed better film quality than that with P(PEGA-co-BuA)TTC. The composites and blank copolymer with P(PEGA-MMA)-TTC exhibited the most rigid behaviour, which might due to the stiffness of the PMMA block. With the presence of the silica, the mechanical properties did not show significant differences, though, the film with the nanofillers were more opaque than the films of the blank copolymers. These behaviours once again along with the results obtained for PAA-

macroRAFT systems confirm the role of the PAA block on the stiffness and the ability to be peeled off of the corresponding copolymers and composites.

DLS was used to determine the particles size and size distribution of the nanocomposites in the emulsion. The results are shown in Table 14

Table 14: DLS study of nanocomposite of PEGA-base macroRAFT agent

Samples	Z-average (nm)	Peak1 (nm) Intensity Percentage(%)	Peak2 Intensity Percentage(%)	PDI
Sicom4	116.2	392.4 (60.1%)	61.1 (39.9%)	0.540
Sicom5	91.09	103 (100%)	-	0.123
Sicom6	134	199.9 (90.9%)	14.66 (8.1%)	0.425
Sicom7	76.94	599 (22.3%)	83.58 (77.7%)	0.380

From the earlier discussions regarding in the preparation of blank copolymers, the copolymerization between the PEGA-TTC macroRAFT agent and MMA was unsuccessful, therefore, the silica would not be encapsulated by the polymers. Sicom5 emulsion showed only 1 peak with Dz = 103 nm thought to be free PMMA particles. The Silica composites prepared with PEGA-TTC (Sicom4, Sicom7) showed a broader distribution than those prepared using PEGA-AA-TTC.

SEM images of nanocomposite of Silica/copolymer 4 and silica/copolymer6 are shown in Figure 27.

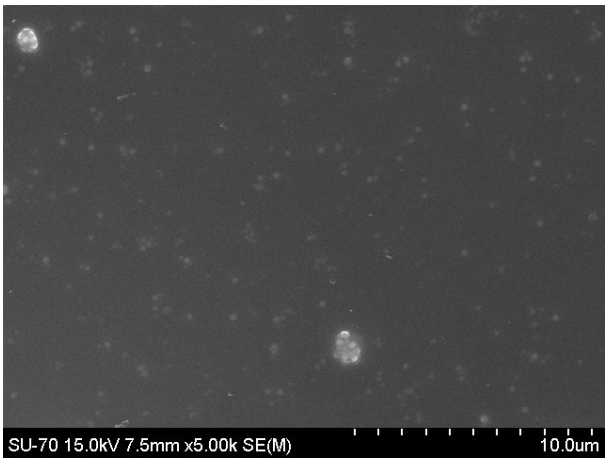

A

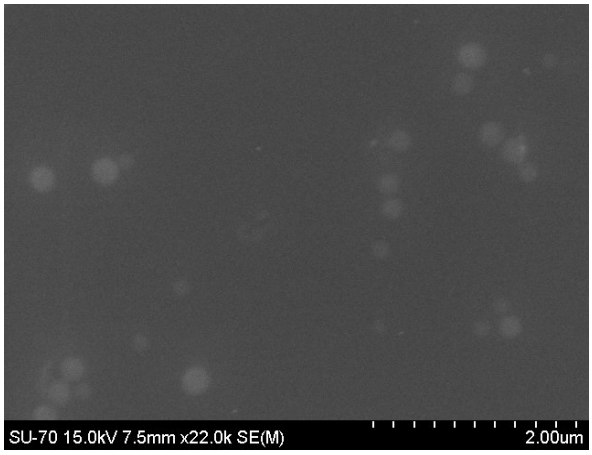

B

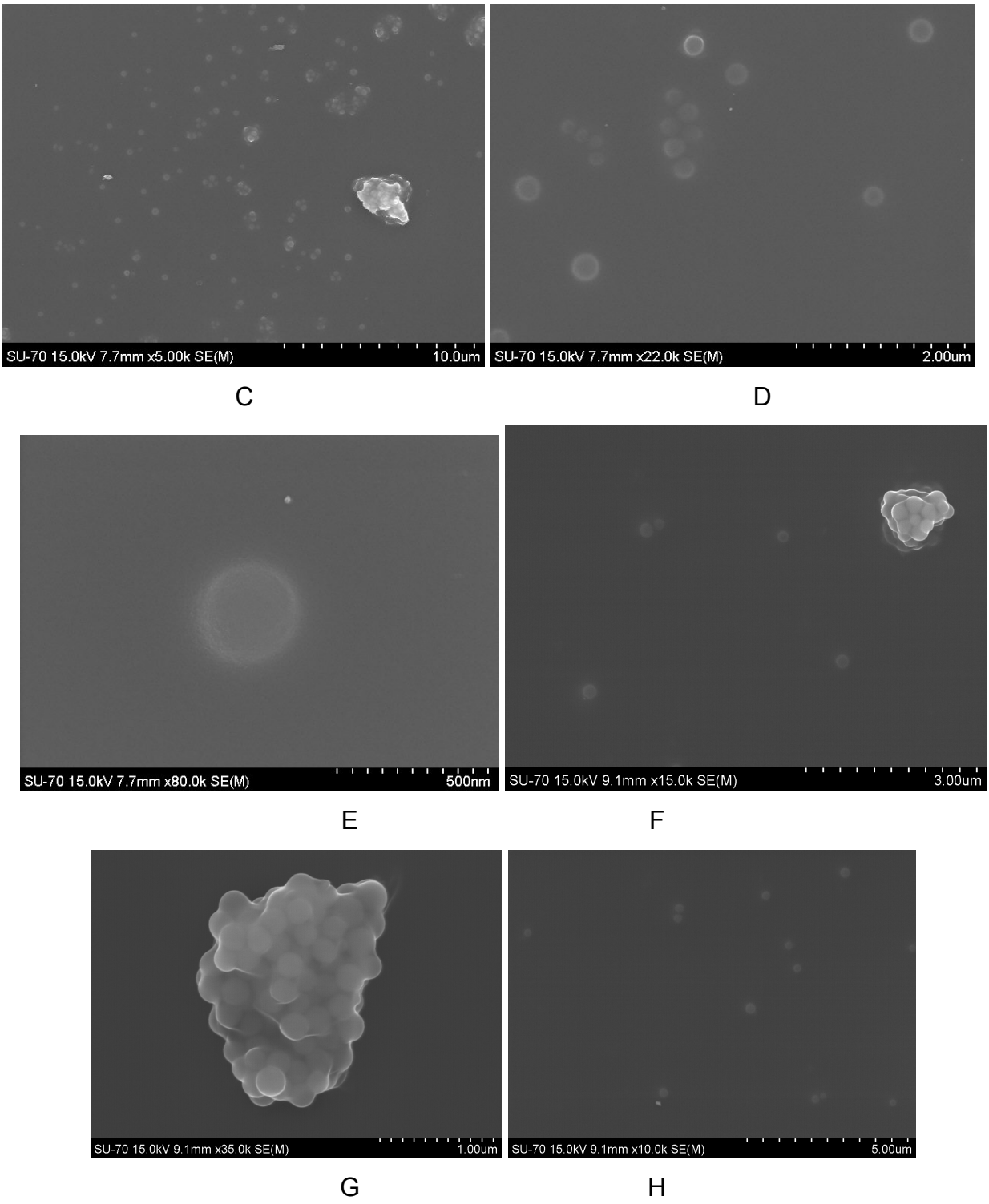

Figure 27: SEM images of nanocomposites: Sicom4 (A and B), Sicom6 (C, D and E), Sicom7 (F, G and H)

From Figure 27 (A) a relatively even distribution of Silica within the matrix is witnessed. Silica nanoparticles with size in the order of 300 nm can be observed isolated although

some clusters are also visible. Figure 27 (E) shows a magnified image of an isolated spherical silica nanoparticle. In the composite using Silica@MPS as nanofillers, the same trend was observed as shown in Figure 27 (F,G,H).

Comparing with the SEM images in Figure 17 of nanocomposite produced using PAA-TTC system, the composites prepared using PEGA-TTC seem to yield better results.

The composite films were characterized by DMA to determine the influence of nanofillers on the Tg of the polymeric part. The results are shown in Table 15 along with the data of the macroRAFT agents and of the corresponding copolymers for comparison.

Table 15: DMA results of the macroRAFT agents, of the blank copolymers and of the corresponding nanocomposites

Samples	**Tg1 (^{o}C)**	**Tg2(^{o}C)**	**Samples**	**Tg1 (^{o}C)**	**Tg2(^{o}C)**
PEGATTC	-60.2	-45.2	PAAPEGATTC	-47.2	x
Copolymer4	-55.5	-43.3	Copolymer6	-46.2	x
Sicom4(SiO2 APS)	-54.7	-41.9	Sicom6 (Si APS)	-45	x
Sicom7 (Si MPS)	-55	-43			

In the case of Sicom 4 and Sicom 7 the results show that in the presence of Silica @ APS, there are slightly increase of the Tg in both butyl acrylate block and PEGA block while in case of Sicom 7 which used silica@MPS seem to yield much less significant changes on the Tg. Hence the difference in the nature of the surface of the silica seems to have difference effect on the Tg of the copolymer.

pH response study of Silica/P(PEGA-AA-BuA) nanocomposites

Composite6 were thought to show pH-response behaviour due to the ability of the acrylic acid repeating units to deprotonate and protonate depending on the pH of the environment. Hence, the Zetasizer was used to measure the Zeta potential of the composite emulsion at varying pH values. The results are shown in Figure 28

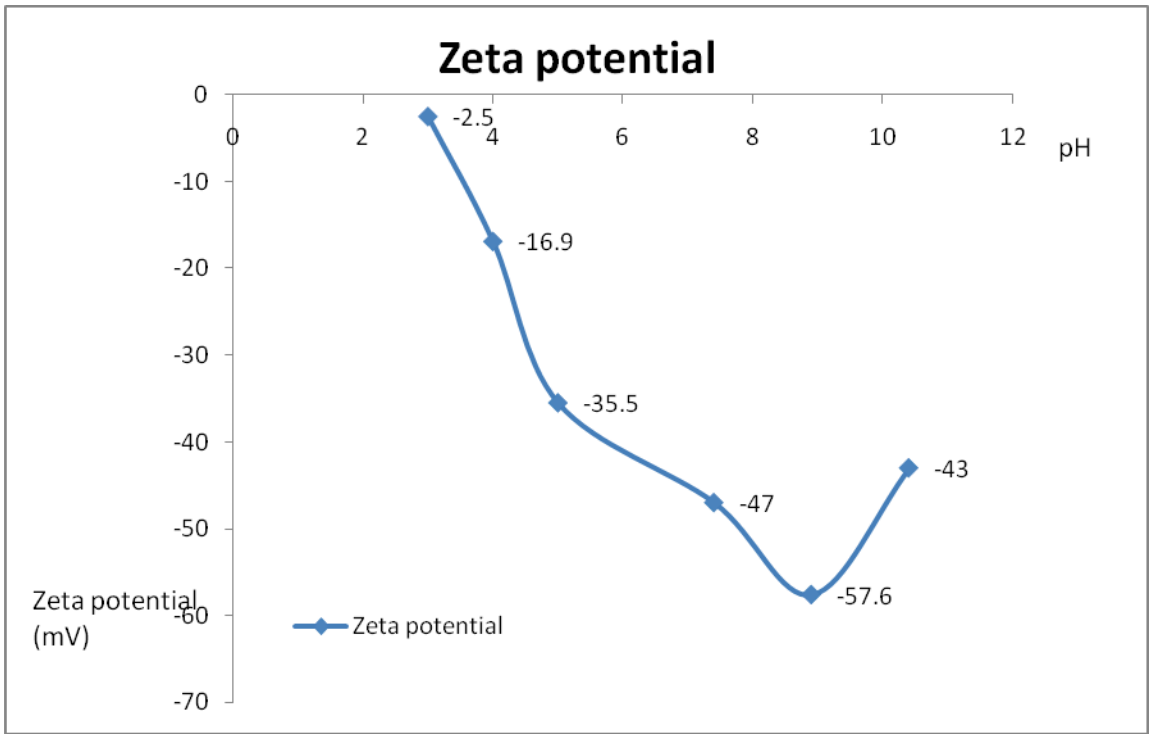

Figure 28: Zeta potential of Sicom6 depending on pH

It can be seen that by changing pH of the emulsion, the Zeta potential values varied. The changing trend of Zeta potential is in agreement with the presumption that the silica nanoparticles are covered by a copolymer with the hydrophilic part containing pH-responsive acrylic acid units at the outer shell as discussed earlier.

4. CONCLUSION

Four macroRAFT agents with different chain lengths and composition were prepared by homopolymerization of acrylic acid (AA), poly(ethylene glycol) methyl ether acrylate (PEGA) using (2-(docdecylthiocarbonothioylthio)-2-methyl propanoic acid (TTC-A) as the chain transfer agent. GPC, ^{1}H-NMR results confirmed the formation of macroRAFT agent with relatively narrow molecular weight distributions.

Copolymerization with butyl acrylate and methyl methacrylate was then carried out under emulsion, surfactant-free condition. Results from DMA, GPC and ^{1}H-NMR revealed the formation of copolymers between macroRAFT agents and butyl acyrate. The copolymers obtained verified the livingness of the systems except in the case of methyl methacrylate which was due to the low blocking effect between acrylate and methacrylate systems. However, the GPC revealed a large difference between the experimental molecular weight and theoretical ones, the polydispersity index showed relatively low values, proving the controlling effect of the RAFT method which indicates that the analytical method needs to be improved.

As regards the thermal behaviour of the polymers, the Tg of butyl acrylate chain was detected in all copolymer samples. The presence of the Tg of the acrylic acid chain depended on the length of the chain, the presence of moisture which acted as plasticizer and the randomness with PEGA. A possible partial blending between butyl acrylate block and acrylic acid block was also suggested to explain the shift of Tg of butyl acrylate to higher temperatures as well as the absence of the acrylic acid block.

The pH-responsive behaviour of the copolymers containing acrylic acid groups was tested by measuring the size and Zeta potential of the emulsion while changing the pH. Copolymer1, copolymer3 and copolymer 6 showed the response regardless of the acrylic acid chain length and distribution.

3-aminopropyl trimethoxylsilane (APS) - surface modified silica nanoparticles and ZnO nanowires were used to prepared nanocomposite using the poly (acrylic acid) macroRAFT agent system. SEM images revealed that ZnO nanowires were aggregated prior to preparation of nanocomposite, thus only Silica nanoparticles (modified with APS and MPS) were used to form hybrid materials with PEGA systems. The formation of nanocomposite was proven by SEM. Poorer distribution of the composite particles in AA systems than in PEGA systems were observed by SEM which may due to the inappropriate chain length and the polyelectrolyte nature of the acrylic acid. DMA results revealed that the Tg of the polymeric parts depends slightly on the presence of the

nanofillers which may hinder the flexibility of the attached hydrophilic groups while enhancing the mobility of the free hydrophobic groups. Silica composites with P(AA-BuA) and P(PEGA-AA-BUA) showed a pH-responsive behaviour, proving that the nanoparticles encapsulation was formed and the hydrophilic polymer layer were at the outer shell of the particles.

5. BIBLIOGRAPHY

1. Ajayan, M., L.S. Schadler, and P. V.Braun, eds. Nanocomposite Science and Technology. 2004, Wiley.
2. Jagur, J. and Grodzinski, eds. Living and controlled polymerization Synthesis,characterization and properties of the respective polymers and copolymers. 2006, Nova Science Publishers, Inc.: New York.
3. Christopher Barner, K., ed. Handbook of RAFT polymerization. 2008, WILEY-VCH.
4. Dos Santos, A.M., T. Le Bris, C. Graillat, F. D'Agosto, and M. Lansalot, Use of a Poly(ethylene oxide) MacroRAFT Agent as Both a Stabilizer and a Control Agent in Styrene Polymerization in Aqueous Dispersed System. Macromolecules, 2009. 42(4): p. 946-956.
5. Dos Santos, A.M., J. Pohn, M. Lansalot, and F. D'Agosto, Combining Steric and Electrostatic Stabilization Using Hydrophilic MacroRAFT Agents in anAb Initio Emulsion Polymerization of Styrene. Macromolecular Rapid Communications, 2007. 28(12): p. 1325-1332.
6. Li, C., J. Han, C.Y. Ryu, and B.C. Benicewicz, A versatile method to prepare RAFT agent anchored substrates and the preparation of PMMA grafted nanoparticles. Macromolecules, 2006. 39(9): p. 3175-3183.
7. Luo, Y.D., I.C. Chou, W.Y. Chiu, and C.F. Lee, Synthesis of PMMA-b-PBA Block Copolymer in Homogeneous and Miniemulsion Systems by DPE Controlled Radical Polymerization. Journal of Polymer Science Part a-Polymer Chemistry, 2009. 47(17): p. 4435-4445.
8. Matsuoka, H., Y. Suetomi, P. Kaewsaiha, and K. Matsumoto, Nanostructure of a poly(acrylic acid) brush and its transition in the amphiphilic diblock copolymer monolayer on the water surface. Langmuir : the ACS journal of surfaces and colloids, 2009. 25(24): p. 13752-62.
9. Prescott, S.W., M.J. Ballard, E. Rizzardo, and R.G. Gilbert, Successful use of RAFT techniques in seeded emulsion polymerization of styrene: Living character, RAFT agent transport, and rate of polymerization. Macromolecules, 2002. 35(14): p. 5417-5425.
10. Stoffelbach, F., L. Tibiletti, J. Rieger, and B. Charleux, Surfactant-Free, Controlled/Living Radical Emulsion Polymerization in Batch Conditions Using a Low Molar Mass, Surface-Active Reversible Addition-Fragmentation Chain-Transfer (RAFT) Agent. Macromolecules, 2008. 41(21): p. 7850-7856.
11. Boyer, C., V. Bulmus, J.Q. Liu, T.P. Davis, M.H. Stenzel, and C. Barner-Kowollik, Well-defined protein-polymer conjugates via in situ RAFT polymerization. Journal of the American Chemical Society, 2007. 129(22): p. 7145-7154.
12. Ali, S.I., J.P. Heuts, B.S. Hawkett, and A.M. van Herk, Polymer encapsulated gibbsite nanoparticles: efficient preparation of anisotropic composite latex particles by RAFT-based starved feed emulsion polymerization. Langmuir : the ACS journal of surfaces and colloids, 2009. 25(18): p. 10523-33.
13. Becer, C.R., S. Hahn, M.W.M. Fijten, H.M.L. Thijs, R. Hoogenboom, and U.S. Schubert, Libraries of methacrylic acid and oligo(ethylene glycol) methacrylate copolymers with LCST behavior. Journal of Polymer Science Part A: Polymer Chemistry, 2008. 46(21): p. 7138-7147.

14. Ferguson, C.J., R.J. Hughes, D. Nguyen, B.T.T. Pham, R.G. Gilbert, A.K. Serelis, C.H. Such, and B.S. Hawkett, Ab initio emulsion polymerization by RAFT-controlled self-assembly. Macromolecules, 2005. 38(6): p. 2191-2204.

15. Hojjati, B. and P.A. Charpentier, Synthesis of TiO2-polymer nanocomposite in supercritical CO2 via RAFT polymerization. Polymer, 2010. 51(23): p. 5345-5351.

16. Houillot, L., C. Bui, M. Save, B. Charleux, C. Farcet, C. Moire, J.A. Raust, and I. Rodriguez, Synthesis of well-defined polyacrylate particle dispersions in organic medium using simultaneous RAFT polymerization and self-assembly of block copolymers. A strong influence of the selected thiocarbonylthio chain transfer agent. Macromolecules, 2007. 40: p. 6500-6509.

17. Rieger, J., G. Osterwinter, C. Bui, F.o. Stoffelbach, and B. Charleux, Surfactant-Free Controlled/Living Radical Emulsion (Co)polymerization ofn-Butyl Acrylate and Methyl Methacrylate via RAFT Using Amphiphilic Poly(ethylene oxide)-Based Trithiocarbonate Chain Transfer Agents. Macromolecules, 2009. 42(15): p. 5518-5525.

18. Sprong, E., J.S.K. Leswin, D.J. Lamb, C.J. Ferguson, B.S. Hawkett, B.T.T. Pham, D. Nguyen, C.H. Such, A.K. Serelis, and R.G. Gilbert, Molecular watchmaking: ab initio Emulsion polymerization by RAFT-controlled self-assembly. Polymers for Africa, 2006. 231: p. 84-93 192.

19. Ferguson, C.J., R.J. Hughes, B.T.T. Pham, B.S. Hawkett, R.G. Gilbert, A.K. Serelis, and C.H. Such, Effective ab initio emulsion polymerization under RAFT control. Macromolecules, 2002. 35(25): p. 9243-9245.

20. Sprong, E., J.S.K. Leswin, D.J. Lamb, C.J. Ferguson, B.S. Hawkett, B.T.T. Pham, D. Nguyen, C.H. Such, G.K. Serelis, and R.G. Gilbert, Molecular watchmaking: ab initio Emulsion polymerization by RAFT-controlled self-assembly. Macromolecular Symposia, 2006. 231: p. 84-93.

21. Rieger, J., F. Stoffelbach, C. Bui, D. Alaimo, C. Jerome, and B. Charleux, Amphiphilic poly(ethylene oxide) macromolecular RAFT agent as a stabilizer and control agent in ab initio batch emulsion polymerization. Macromolecules, 2008. 41(12): p. 4065-4068.

22. Boisse, S., J. Rieger, K. Belal, A. Di-Cicco, P. Beaunier, M.-H. Li, and B. Charleux, Amphiphilic block copolymer nano-fibers via RAFT-mediated polymerization in aqueous dispersed system. Chem Commun (Camb), 2010. 46(11): p. 1950-2.

23. Wi, Y., K. Lee, B. Lee, and S. Choe, Soap-free emulsion polymerization of styrene using poly(methacrylic acid) macro-RAFT agent. Polymer, 2008. 49(26): p. 5626-5635.

24. Pham, B.T.T., H. Zondanos, C.H. Such, G.G. Warr, and B.S. Hawkett, Miniemulsion Polymerization with Arrested Ostwald Ripening Stabilized by Amphiphilic RAFT Copolymers. Macromolecules, 2010. 43(19): p. 7950-7957.

25. Beija, M., J.-D. Marty, and M. Destarac, RAFT/MADIX polymers for the preparation of polymer/inorganic nanohybrids. Progress in Polymer Science, 2011. 36(7): p. 845-886.

26. Liu, J., L. Zhang, S. Shi, S. Chen, N. Zhou, Z. Zhang, Z. Cheng, and X. Zhu, A Novel and Universal Route to SiO2-Supported Organic/Inorganic Hybrid Noble Metal Nanomaterials via Surface RAFT Polymerization. Langmuir : the ACS journal of surfaces and colloids, 2010. 26(18): p. 14806-14813.

27. Esteves, A.C.C., P. Hodge, T. Trindade, and A.M.M.V. Barros-Timmons, Preparation of nanocomposites by reversible addition-fragmentation chain transfer polymerization from

the surface of quantum dots in miniemulsion. Journal of Polymer Science Part A: Polymer Chemistry, 2009. 47(20): p. 5367-5377.

28. Daigle, J.-C. and J.P. Claverie, A Simple Method for Forming Hybrid Core-Shell Nanoparticles Suspended in Water. Journal of Nanomaterials, 2008. 2008: p. 1-8.

29. Gang M., X.F., Weiwei D., Ruhua T., Yiping Z., Zanhong D., Shu Z., Jingzhen S., Liang L., One step synthesis of vertically aligned ZnO nanowirearrays with tunable length. Applied Surface Science 2010. 256: p. 6543–6549.

30. Lin, C. and Y. Li, Synthesis of ZnO nanowires by thermal decomposition of zinc acetate dihydrate. Materials Chemistry and Physics, 2009. 113(1): p. 334-337.

31. Stober, W., A. Fink, and E. Bohn, CONTROLLED GROWTH OF MONODISPERSE SILICA SPHERES IN MICRON SIZE RANGE. Journal of Colloid and Interface Science, 1968. 26(1): p. 62-&.

32. Bogush, G.H., M.A. Tracy, and C.F. Zukoski, PREPARATION OF MONODISPERSE SILICA PARTICLES - CONTROL OF SIZE AND MASS FRACTION. Journal of Non-Crystalline Solids, 1988. 104(1): p. 95-106.

33. Bogush, G.H. and C.F. Zukoski, STUDIES OF THE KINETICS OF THE PRECIPITATION OF UNIFORM SILICA PARTICLES THROUGH THE HYDROLYSIS AND CONDENSATION OF SILICON ALKOXIDES. Journal of Colloid and Interface Science, 1991. 142(1): p. 1-18.

34. Tan, C.G., B.D. Bowen, and N. Epstein, Production of monodisperse colloidal silica spheres-effect of temperature. Journal of Colloid and Interface Science, 1987. 118(1): p. 290-293.

35. John, V.T., B. Simmons, G.L. McPherson, and A. Bose, Recent developments in materials synthesis in surfactant systems. Current Opinion in Colloid & Interface Science, 2002. 7(5-6): p. 288-295.

36. Antonietti, M., Surfactants for novel templating applications. Current Opinion in Colloid & Interface Science, 2001. 6(3): p. 244-248.

37. Wang, W., B.H. Gu, and L.Y. Liang, Effect of surfactants on the formation, morphology, and surface property of synthesized SiO2 nanoparticles. Journal of Dispersion Science and Technology, 2004. 25(5): p. 593-601.

38. Jeon, B.J., H.J. Hah, and S.M. Koo, Surface modification of silica particles with organoalkoxysilanes through two-step (acid-base) process in aqueous solution. Journal of Ceramic Processing Research, 2002. 3(3): p. 216-221.

39. Bourgeat-Lami, E. and J. Lang, Encapsulation of inorganic particles by dispersion polymerization in polar media - 1. Silica nanoparticles encapsulated by polystyrene. Journal of Colloid and Interface Science, 1998. 197(2): p. 293-308.

40. Jesionowski, T., F. Ciesielczyk, and A. Krysztafkiewicz, Influence of selected alkoxysilanes on dispersive properties and surface chemistry of spherical silica precipitated in emulsion media. Materials Chemistry and Physics, 2010. 119(1-2): p. 65-74.

41. Carvalho, R., Encapsulation of SiO_2 coated Gd_2O_3: Eu^{3+}nanoparticles using PAA macroRAFT agents. 2010.

42. Laurence Couvreur, Catherine Lefay, Joe Belleney, Bernadette Charleux, Olivier Guerret, and a.S.p. Magnet, First Nitroxide-Mediated Controlled Free-Radical Polymerization of Acrylic Acid. Macromolecules, 2003. 36: p. 8260-8267.

43. Timmons, A.B. and B.C. UPMC, [unpublished data].

44. Akira Hirao, Y.I., and Seiichi Nakahama, Protection and Polymerization of Functional Monomers. 11. Synthesis of Well-Defined Poly(4-vinylbenzoic acid) by Means of Anionic Living Polymerization of 2- (4-Vinylphenyl)-4,4-dimethyl-2-oxazol. Macromolecules, 1988. 21: p. 561-565

45. http://www.polymerprocessing.com/polymers/PBA.html.

46. Maurer, J.J., D.J. Eustace, and C.T. Ratcliffe, THERMAL CHARACTERIZATION OF POLY(ACRYLIC ACID). Macromolecules, 1987. 20(1): p. 196-202.

47. Hong, C.-Y., X. Li, and C.-Y. Pan, Fabrication of smart nanocontainers with a mesoporous core and a pH-responsive shell for controlled uptake and release. Journal of Materials Chemistry, 2009. 19(29): p. 5155.

48. Schneider, G.g. and G. Decher, Functional Core/Shell Nanoparticles via Layer-by-Layer Assembly. Investigation of the Experimental Parameters for Controlling Particle Aggregation and for Enhancing Dispersion Stability. Langmuir 2008. 24: p. 1778-1789.

49. Devon A. Shipp, J.-L.W., and Krzysztof Matyjaszewski, Synthesis of Acrylate and Methacrylate Block Copolymers Using Atom Transfer Radical Polymerization. Macromolecules, 1998. 31: p. 8005 8008.

ANNEX

Annex 1: FT-IR of P(AA)TTC

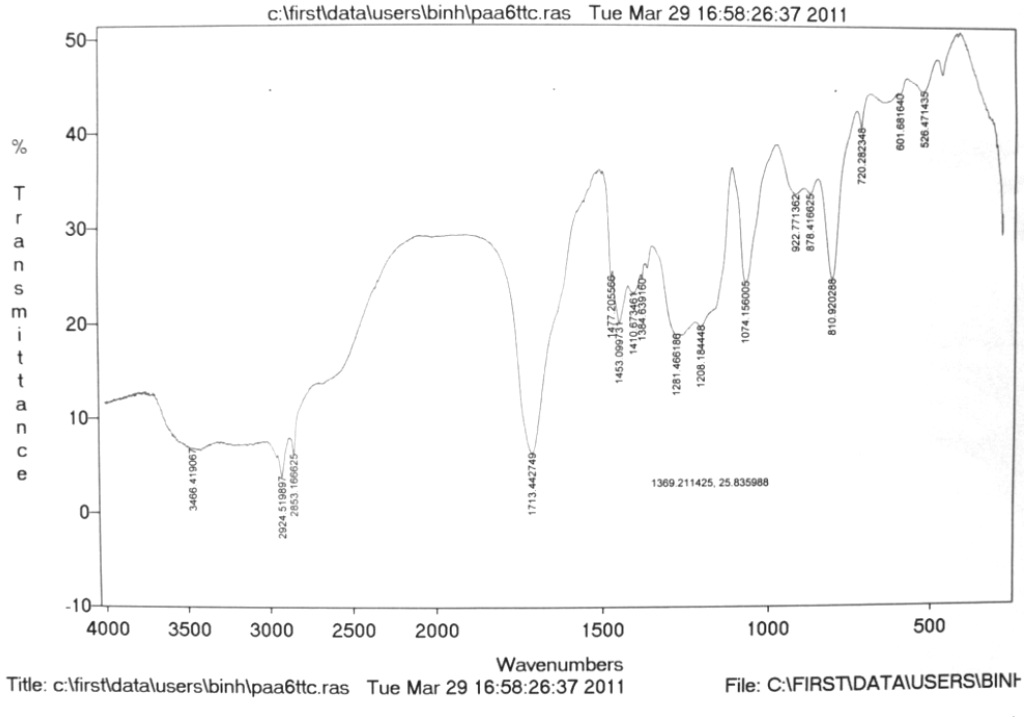

Annex 2: FT-IR of P(AA-co-BuA)TTC

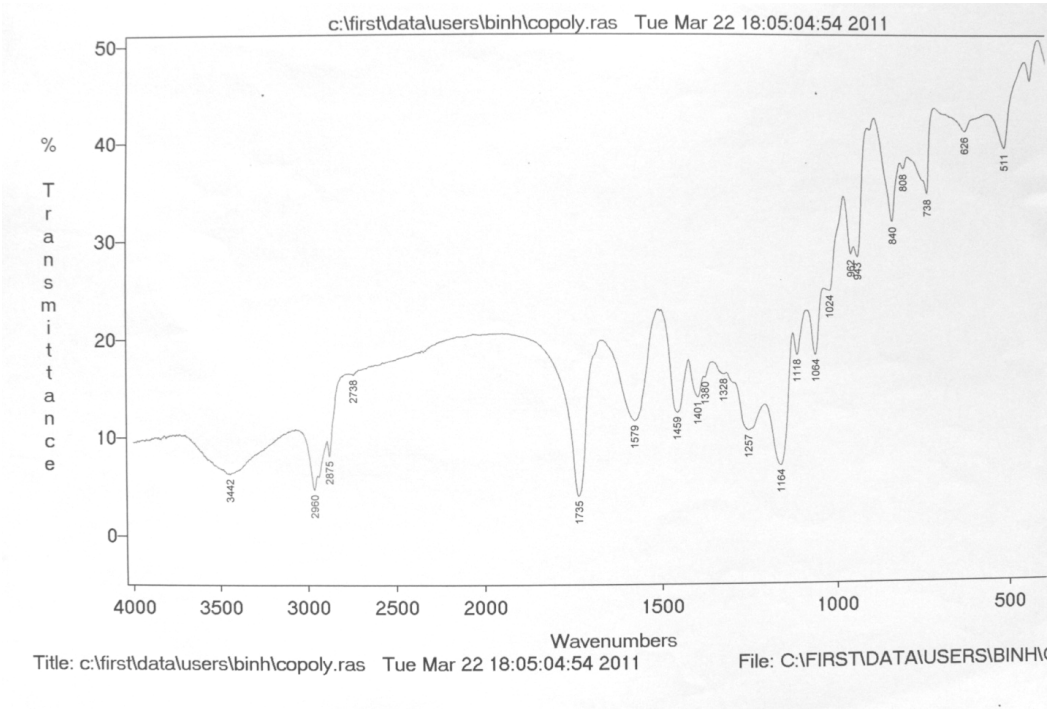

Annex 3: FT-IR of PEGA monomer

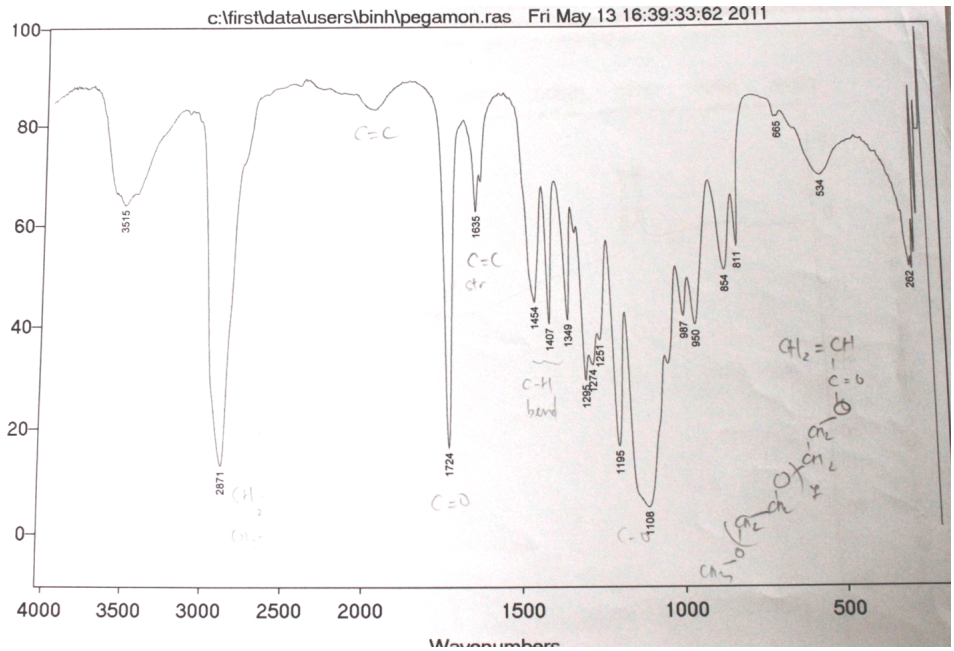

Annex 4: FT-IR of PEGA-TTC

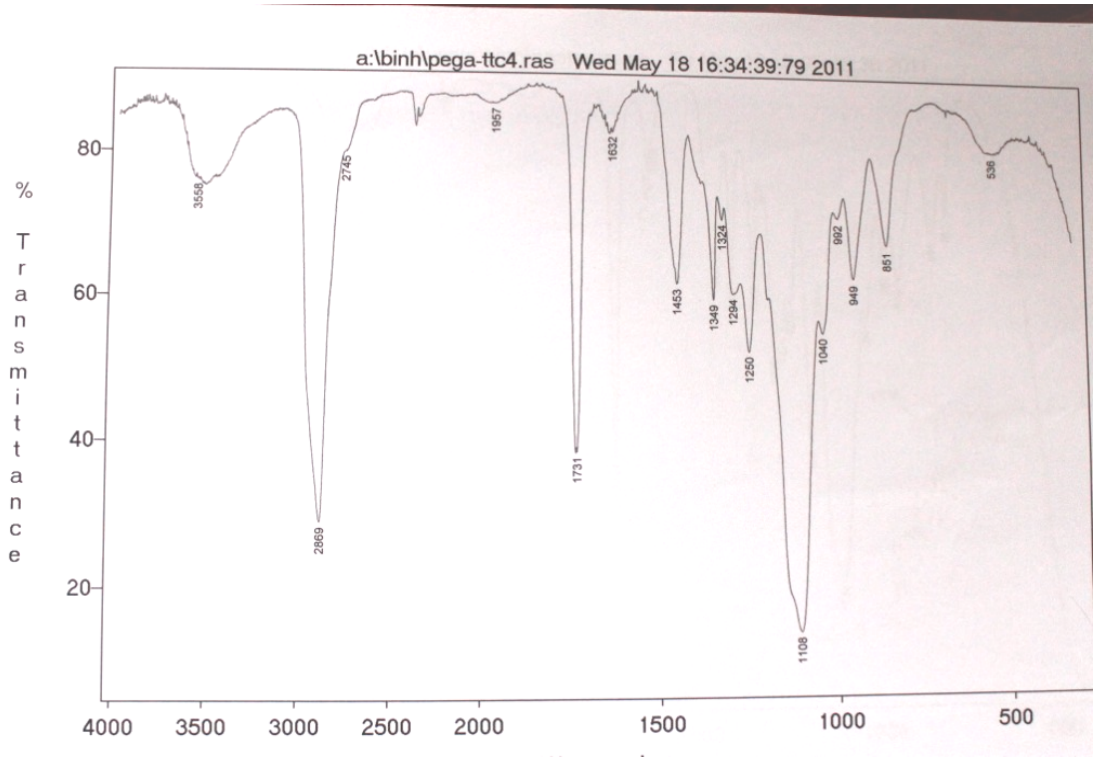

Annex 5: Proton NMR of Copolymer4 P(PEGA-BuA)TTC

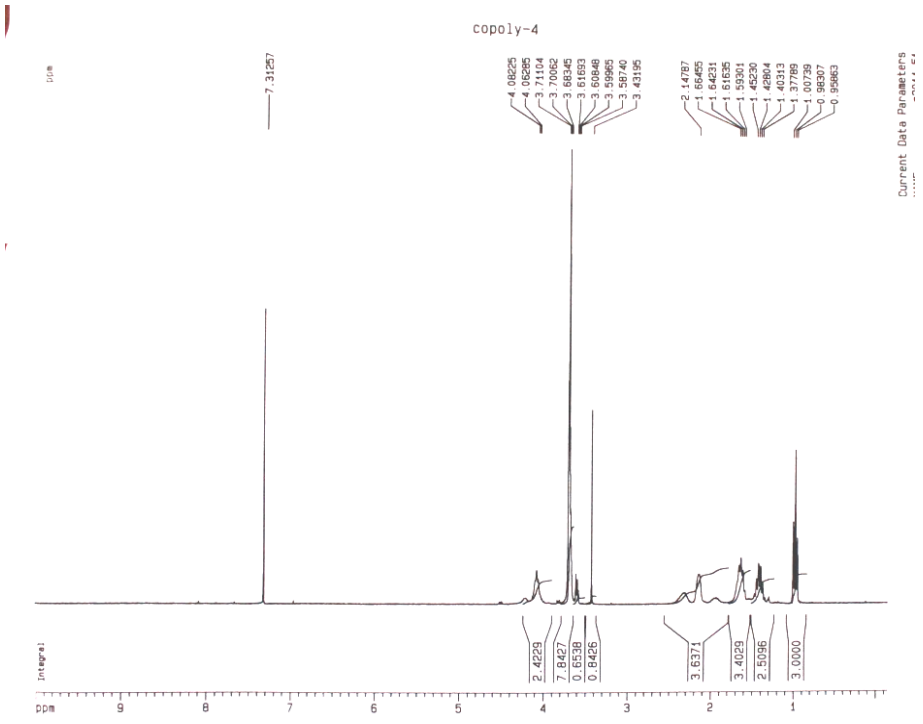

Annex 6: Proton NMR of copolymer6 P(AA-PEGA-BuA)TTC